AFRL-VA-WP-TR-2003-3073

SURVIVABILITY OF AFFORDABLE AIRCRAFT COMPOSITE STRUCTURES

Volume 3: Characterization of Affordable Woven Carbon/Epoxy Composites Under Low-Velocity Impact Loading

Dr. Mahesh V. Hosur and Dr. Shaik Jeelani

Tuskegee University
Center for Advanced Materials
Tuskegee, AL 36088

Dr. Uday K. Vaidya
The University of Alabama in Birmingham

Dr. Ajit D. Kelkar
North Carolina A&T State University

APRIL 2003

Final Report for 01 October 1999 – 01 March 2003

STINFO FINAL REPORT

AIR VEHICLES DIRECTORATE
AIR FORCE RESEARCH LABORATORY
AIR FORCE MATERIEL COMMAND
WRIGHT-PATTERSON AIR FORCE BASE, OH 45433-7542

NOTICE

USING GOVERNMENT DRAWINGS, SPECIFICATIONS, OR OTHER DATA INCLUDED IN THIS DOCUMENT FOR ANY PURPOSE OTHER THAN GOVERNMENT PROCUREMENT DOES NOT IN ANY WAY OBLIGATE THE U.S. GOVERNMENT. THE FACT THAT THE GOVERNMENT FORMULATED OR SUPPLIED THE DRAWINGS, SPECIFICATIONS, OR OTHER DATA DOES NOT LICENSE THE HOLDER OR ANY OTHER PERSON OR CORPORATION; OR CONVEY AND RIGHTS OR PERMISSION TO MANUFACTURE, USE, OR SELL ANY PATENTED INVENTION THAT MAY RELATE TO THEM.

THIS REPORT HAS BEEN REVIEWED BY THE OFFICE OF PUBLIC AFFAIRS (ASC/PA) AND IS RELEASABLE TO THE NATIONAL TECHNICAL INFORMATION SERVICE (NTIS). AT NTIS, IT WILL BE AVAILABLE TO THE GENERAL PUBLIC, INCLUDING FOREIGN NATIONS.

THIS TECHNICAL REPORT HAS BEEN REVIEWED AND IS APPROVED FOR PUBLICATION.

/s/
ARNOLD H. MAYER
Project Engineer
Design and Analysis Methods Branch
Structures Division

/s/
MICHAEL L. ZEIGLER, Chief
Design and Analysis Methods Branch
Structures Division

/s/
DAVID M. PRATT, PhD
Technical Advisor
Structures Division

COPIES OF THIS REPORT SHOULD NOT BE RETURNED UNLESS RETURN IS REQUIRED BY SECURITY CONSIDERATIONS, CONTRACTUAL OBLIGATIONS, OR NOTICE ON A SPECIFIC DOCUMENT.

REPORT DOCUMENTATION PAGE

Form Approved
OMB No. 0704-0188

1. REPORT DATE *(DD-MM-YY)*	2. REPORT TYPE	3. DATES COVERED *(From - To)*
April 2003	Final	10/01/1999 – 03/01/2003

4. TITLE AND SUBTITLE

SURVIVABILITY OF AFFORDABLE AIRCRAFT COMPOSITE STRUCTURES

Volume 3: Characterization of Affordable Woven Carbon/Epoxy Composites Under Low-Velocity Impact Loading

5a. CONTRACT NUMBER F33615-99-C-3608

5b. GRANT NUMBER

5c. PROGRAM ELEMENT NUMBER 62201F

6. AUTHOR(S)

Dr. Mahesh V. Hosur and Dr. Shaik Jeelani (Tuskegee University)
Dr. Uday K. Vaidya (The University of Alabama in Birmingham)
Dr. Ajit D. Kelkar (North Carolina A&T State University)

5d. PROJECT NUMBER 2402

5e. TASK NUMBER SA

5f. WORK UNIT NUMBER AC

7. PERFORMING ORGANIZATION NAME(S) AND ADDRESS(ES)

Tuskegee University
Center for Advanced Materials
Tuskegee, AL 36088

The University of Alabama in Birmingham
North Carolina A&T State University

8. PERFORMING ORGANIZATION REPORT NUMBER

9. SPONSORING/MONITORING AGENCY NAME(S) AND ADDRESS(ES)

Air Vehicles Directorate
Air Force Research Laboratory
Air Force Materiel Command
Wright-Patterson Air Force Base, OH 45433-7542

10. SPONSORING/MONITORING AGENCY ACRONYM(S) AFRL/VASD

11. SPONSORING/MONITORING AGENCY REPORT NUMBER(S) AFRL-VA-WP-TR-2003-3073

12. DISTRIBUTION/AVAILABILITY STATEMENT

Approved for public release; distribution is unlimited.

13. SUPPLEMENTARY NOTES

This is volume 3 of three. See also AFRL-VA-WP-TR-2003-3071 and AFRL-VA-WP-TR-2003-3072. This report contains color.

14. ABSTRACT *(Maximum 200 Words)*

Experimental investigations carried out on affordable woven carbon/epoxy laminates under low-velocity impact loading are reported in this volume. Stitched and unstitched carbon/epoxy laminates were fabricated using plain and satin weave fabric with SC-15 epoxy resin system. Two orthogonal stitch spacing: 12.7- and 15.4-mm were used. Four-inch square samples were subjected to low-velocity impact loading at energy ranging from 5-40 J. Results of the study indicated that the damage due to low-velocity impact loading reduced considerably due to stitching. Of the two weave types, satin weave laminates carried higher impact loads compared to plain weave laminates due to relatively straighter fiber architecture.

In another study, effects of laminate thickness and samples size on the upper and lower-bound energy level were established. To establish damage tolerance of woven fabric composites, post impact studies were carried out which included static compression and fatigue tests. Post fatigue tension tests were carried out to determine the reduction in stiffness. Though most of the laminates sustained 100,000 fatigue cycles, there was a sharp decrease in the stiffness with increasing drop height.

15. SUBJECT TERMS Affordable Woven Composites, Low-Velocity Impact Loading, Nondestructive Evaluation, Damage Tolerance, Post Impact Compression, Post-Impact Fatigue

16. SECURITY CLASSIFICATION OF:			17. LIMITATION OF ABSTRACT:	18. NUMBER OF PAGES	19a. NAME OF RESPONSIBLE PERSON (Monitor)
a. REPORT	b. ABSTRACT	c. THIS PAGE			Arnold Mayer
Unclassified	Unclassified	Unclassified	SAR	62	19b. TELEPHONE NUMBER *(Include Area Code)* (937) 255-5232

Standard Form 298 (Rev. 8-98)
Prescribed by ANSI Std. Z39-18

Table of Contents

List of Figures

Figure **Page**

List of Figures (Continued)

Figure **Page**

List of Tables

Table **Page**

1. Studies on Impact Damage Resistance of Affordable Stitched Woven Carbon/Epoxy Composite Laminates

This section discusses the response of seven-layer plain and satin weave carbon fabric-reinforced composites fabricated using a low-cost vacuum assisted resin infusion molding (VARIM) process under low-velocity impact loading. Both stitched and unstitched laminates were tested at energy levels ranging 5–50 J using an instrumented drop-weight machine. A three-cord Kevlar thread was used to stitch the laminate in two orthogonal grid patterns each at a 6-mm pitch: one with 25.4-mm and the other with 12.7-mm grid. Damage due to impact loading was evaluated through ultrasonic nondestructive evaluation (NDE). Results of the study showed the effectiveness of stitching in containing the damage size with 12.7-mm grid stitch samples exhibiting the least damage. Further, satin weave fabric composites exhibit better impact resistance as compared to plain weave fabric composites.

1.1 Introduction

Fiber-reinforced plastic (FRP) composites exhibit high specific strength and stiffness as compared to conventional metallic components. Of different types of FRP composites, carbon/epoxy laminates are most used in weight-sensitive aerospace industry as they offer highest specific strength and stiffness. However, the increased use of carbon/epoxy reinforced plastic (CFRP) composites in many applications has been hindered due to concerns of the complex failure modes intrinsic to composite materials. The primary concern with the current conventional CFRP materials is premature failure due to delamination under transverse loading. Conventional composite materials, which consist of laminated layers of unidirectional fibers embedded in matrix, are very strong in the direction of fibers, but much weaker in the direction perpendicular to the fibers. Out-of-plane properties of a unidirectional composite laminate are matrix dominated. Delaminations are usually initiated in one of the three ways: by means of mechanical defects in the composite, damage due to impact, or out-of-plane loads. In all of these cases development of through-the-thickness stress is the primary cause of delamination.

When subjected to impact loading, inelastic energy in composites is absorbed in the form of creation of new surfaces. The failure mechanisms include matrix cracking, delamination, and ply splitting [1-8], all of which reduce the residual mechanical properties of the laminate considerably. The worst scenario occurs when the damage is at subsurface levels. It is well known that the residual compressive strength, which is the most affected mechanical property, is reduced up to 50 percent [9-13]. Hence, in past couple of decades material science researchers have invested their efforts to address the delamination issues. Methods of reducing interply delamination include the use of tougher matrix systems, woven fabrics, and through-thickness reinforcement. The main methods of through-thickness reinforcement include 3-D weaving, pinning, and stitching, of which stitching has been demonstrated to be most effective in improving the delamination resistance [14-25]. The early attempts of improving delamination resistance were made by Huang et al. [14] in the late 1970s where steel wires of 0.33 mm diameter were placed at $\pm 45^{\circ}$ angles to the thickness of the laminate separated by 1.6 mm. But embedding the steel wires by hand was not practical. In the mid 1980s Mignery et al. [15] explored the possibility of stitching fiber threads in to the fabric preform before curing of the resin. As per Kang and Lee [16], the stitched composite laminate tolerates out-of-plane load and absorbs more energy during interlaminar crack growth, due to

which the damage area is restricted and the integrity of the structure is preserved. Further, stitching appears to be the most cost-effective process for manufacture of damage-tolerant composite structures.

Another issue that limits the usage of composite structures is cost. Currently, composite components in aerospace industry are mostly made of unidirectional laminates fabricated using prepregs. Prepregs are expensive materials and require stringent storage requirements, and expensive manufacturing process like autoclave molding. In addition, prepregs have limited shelf life. Also, any innovative concepts like through-the-thickness stitching are difficult to incorporate. While prepregs are very useful in forming simple folds and curves and to produces T-, L- and I- shaped components, they are not very attractive for complex curvatures. If complex structural components are to be made of unidirectional prepregs, they have to be produced from smaller, simple parts, which increase the cost of assembly. Over 70 percent of the cost of composite structures is due to assembly and layup [26]. Further, the cost of the prepreg scrap is about 40 percent of the fabric cost (less than 2/3 of the purchased prepreg ends up on the component). Hence, manufacturers and potential users of advanced composites are adopting alternative approaches. As such, liquid molding processes offer great potential for reducing layup and assembly costs. One such technique is the VARIM process [27, 28]. By using dry woven fabrics, it is possible to produce complex 3-D performs due to greater drapability of the fabric. There is a direct route to manufacturing with fewer parts. Such integrated parts reduce the cost associated with tooling, layup operations, part counts, and fasteners. The added advantages include increased dimensional tolerance, outlife of raw materials (fibers), reduced cycle times, near net molded components, reduced post-molding process, and less material scrap.

Studies on the behavior of woven fabric composites under impact loading are limited [29-33]. Most of the literature on the woven composites is related to predicting the elastic and static strength properties. Impact studies on woven composites used in aircraft applications are important for obvious reasons. Wu [29] conducted progressive studies on woven composites. However, Wu's progressive study involved ranging the impact velocities from low to ballistic speeds and energies. Naik et al. [30] conducted a study on the behavior of unidirectional and woven fabric laminates under low-velocity impact using a 3-D transient finite element code and a failure function based on Tsai-Hill criterion. They observed that the failure function is lower for woven fabric laminates than for unidirectional laminates, indicating that woven laminates are more resistant to impact damage. Naik et al. [31,32] also undertook an investigation to study the damage initiation behavior in polymer matrix woven fabric composite plates subjected to a transverse central low-velocity impact using modified Hertz contact law and a 3-D transient finite element analysis. Walsh et al. [33] conducted studies to examine the deformation and penetration failure mechanisms of plain weave Spectra polyethylene fiber/vinyl ester and polyurethane resin matrix composites.

Since liquid molding is still an emerging technology, the data on woven-fabric-reinforced plastic laminates made using this process is lacking. Especially, if the woven fabric composite laminates made using liquid molding processes are to be used with confidence for critical structural component applications, investigations have to be carried out to characterize them under various loading conditions. Hence, in the current research work, experimental investigations were carried out to manufacture composite laminates using

VARIM with plain as well as satin weave fabric reinforcement. In addition, through-the-thickness stitching with high-strength Kevlar thread was employed to enhance the damage resistance. Two stitch densities 25.4 and 12.7-mm grid–were used. The laminates were subjected to low-velocity impact loading at energies ranging from 5– 50J using an instrumented impact testing machine. The transient response of the sample was recorded and analyzed. Damage due to impact loading was determined using NDE technique. Results of the study are discussed in terms of peak load, absorbed energy, and damage area as a function of impact energy as well as the fabric architecture.

1.2 Experimental Work

1.2.1 Low Cost Manufacturing

Improving the manufacturing technology is the greatest challenge today in the field of composites. Methods of manufacturing materials that are chosen for their special mechanical properties should be built upon the principle of optimization of the physical properties of those materials. Thus, the main issue regarding the manufacturing of different materials is the compromise between the cost of the manufacturing process and the strength of material obtained from that process. VARIM is a simplified and environmentally responsible method of processing. The process uses one-sided low-cost tooling and vacuum bag technology. In this process, resin is brought on to the preform through a leaky pipe and is pulled by vacuum. A high-permeability membrane is placed on top of the preform, which allows the resin to flow freely on top and seep through the thickness of fabric layers. The process is generally carried out at room temperature if viscosity constraints are not a limiting factor. Due to the specifics of the process, parts are generally of lower void content and uniform structure than with other related processes. It is efficient and cost effective as it has a high production rate and the process control is easier. Further, it is more flexible, produces consistent quality parts, requires minimum cleanup, and enables fabrication of large, complex parts. Parts with inserts, integrated stiffeners, curvatures, and bondlines are easy to manufacture.

In the current investigations, composite panels were fabricated using seven layers of plain and 8eight-harness satin carbon fabric and SC-15 epoxy resin system. Plain weave carbon fabric was of style 4060-6 with 10 oz/sq yard and satin weave was eight harness carbon fabric of style 5999 with 10.8 oz/sq yard supplied by Fiber Materials Inc. Through-the-thickness stitching was performed on perform by a stitching machine using a three cord Kevlar thread with a pitch of 6 mm. Three types of stitch/unstitch configurations were used: 1) unstitched, 2) stitched with 25.4-mm spacing, and 3) stitched with 12.7-mm spacing.

For fabricating the laminate (size 60 by 90 cm), a release film was applied to the mold. Seven layers were carefully placed on the mold. Then a sealant tape was tacked on the surface of the mold about 50 mm from the perimeter of the fabric layers. Resin supply tubes were connected to the system with the mold end of the tube connected to a spiral wrap, which distributed the resin through the laminate when vacuum was applied. Tubes linking the vacuum pump and the spiral wrap were also connected. A resin trap was placed between the vacuum pump and the mold to collect any excess resin. Finally, the vacuum bag was placed on the mold and pressed firmly against the sealant tape to provide an airtight system. The preform was left to debulk under vacuum to remove any entrapped air within the dry fabric. After debulking, the SC-15 resin system was infused. The inlet valve was closed when resin

completely wetted the preform and reached the suction side. The wet laminate was left to cure at room temperature. Vacuum was maintained until the end of cure to remove any volatiles generated during the polymerization, and also to maintain the pressure. Figure 1 illustrates the arrangements for the fabrication process.

Figure 1. Fabrication of Laminate by VARIM Process

1.2.2 Low-velocity Impact Testing

Impact tests in this study were conducted using an instrumented impact testing system (DYNATUP model 8210, Figure 2), which consists of a drop tower equipped with an impactor and a variable crosshead weight arrangement, a high-speed data acquisition system, and a load transducer mounted in the impactor. The crosshead/impactor weight was kept constant at 6.33 Kg for all tests. The specimen support fixture at the bottom of the drop tower facilitates circular clamped condition with a clear span of 75 mm. The falling weight is guided through two smooth columns. The impactor end is fitted with an instrumented tup of 15.56 kN capacity that records the transient response of the specimen. Transient response of the sample includes velocity, deflection, load, and energy as function of time. A total of 4096 data points are collected during the impact event. The machine is fitted with a velocity detector that measures the velocity of the tup just before it strikes the specimen, which also triggers data collection. The pneumatic rebound brakes prevent multiple impacts. In the current study, specimens of size 90 by 90 mm were used and were tested at energy levels ranging 5–50 J, which represent the range that a typical aircraft structure experiences under low-velocity impact situations. Load-time response was plotted for each sample.

1.2.3 Ultrasonic NDE

Ultrasonic inspection of the laminate was conducted using a Krautkramer ultrasonic pulser receiver unit with TestTech mechanical system. The scanning was done in pulse-echo immersion mode using a 5-MHz 25.4-mm point focus sensor. Scanning was done with the

impacted surface facing the sensor to obtain the projected damage. The gate was set on the back surface echo. All of the laminates were subjected to ultrasonic NDE both before and after impact testing. The ultrasonic testing before impact loading was carried out to ensure that there was no fabrication defect in the sample. Post-impact ultrasonic testing was conducted to evaluate the extent of damage in the sample. From the C-scan images, the damage area as projected onto a plane was measured.

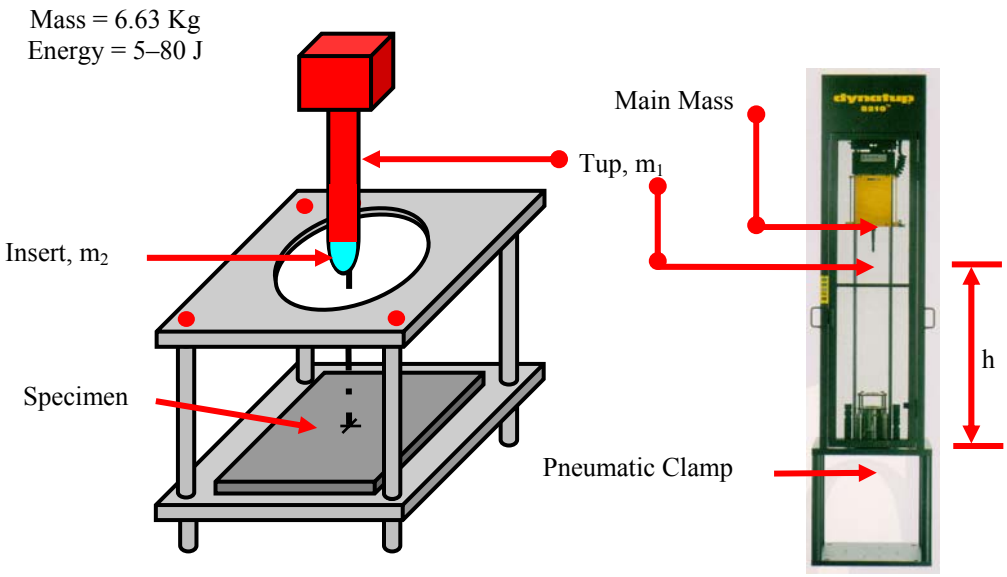

Figure 2. Instrumented Drop-Weight Impact Setup

1.3 Results and Discussion

Samples were subjected to impact loading at 11 energy levels ranging from 5–50 J. The dynamic response of each sample is recorded and analyzed. From the data acquisition system, load, time, energy, velocity and deflection data are recorded. In all, 4096 data points are acquired over the impact duration. The data is analyzed in terms of peak load and absorbed energy. The absorbed energy is calculated as the difference of total energy (at the end of the event) and the energy at peak load. The impact energy is, in general, mainly absorbed in the form of elastic deformation, plastic deformation, and through various damage modes. As composite materials have no plastic deformation all of the energy is absorbed through elastic deformation and through different failure modes. Hence, in the current study, absorbed energy is attributed to the energy spent in creating damage.

1.3.1 Plain Weave Carbon/Epoxy Composite

The results of impact tests on plain weave carbon/epoxy laminates are presented in Table 1. Further, impact damage area as measured from the ultrasonic c-scan is also presented. Figure 3, illustrates the impact response of unstitched laminate at energy levels ranging from 5–40 J. Some representative ultrasonic c-scan images with the photographs of front and back surface of the laminates impacted at 10, 20, and 40 J respectively are presented in Figures 4 a-c.

Impact testing was not carried out beyond 40 J as there was total penetration of the sample at 40 J. It can be seen from the plot in Figure 3 that the peak load increases with increase in impact energy. The slope of the load-time curve, which is designated as the contact stiffness increases with energy. The absorbed energy increases with an increase in impact energy. At 5 J, the loading and unloading portions of the curve are smooth and symmetric, indicating that there is little damage. Though there was no discernable damage from the transient response curves, ultrasonic study revealed the presence of damage local to the point of loading. At 7.5 J small oscillations in the transient load were observed, which can be attributed to the damage initiation and growth. At 10 J, there was barely a visible dent at the surface, though no indication of damage was seen at the back surface. However, ultrasonic studies did reveal increasing damage due to contact stresses. At 15 and 20 J, there was a clear dent at the point of impact and a sudden increase in the impact damage with more than a third of impact energy being absorbed through damage. This indicates that up to 20 J, the damage in the laminate was basically limited to the impact point due to the contact stresses, and the flexural tensile stresses were well within the failure limits. The first backface damage was observed at 25 J with more than 50 percent of the impact energy going in the creation of damage. This also indicates the energy level at which there is saturation of load that the laminate was able to sustain. At 30 and 35 J, there was partial penetration with 60-65 percent of impact energy being absorbed through damage. At 40 J, there is complete penetration of the sample, indicated by the sharp drop in the load-time response. However, in all of the cases where there was extensive damage, the damage was restricted to the region very close to the impact location and was symmetric. Again, there is notable difference in the response of woven fabric laminates as compared to the unidirectional laminates. Due to the interlacing of the weave, the lowermost ply in woven fabric laminates does not split, which is very common in unidirectional laminate. The weave accommodates most of the energy by supporting the fibers in both directions from failing. This results in total suppression of delamination. Further, the damage is localized. This will result in very little drop in the residual in-plane properties. In the case of unidirectional laminates, delamination is the major failure mode, which is indicated by a sudden drop in load. Further, in unidirectional laminates, delamination damage, once initiated, progresses rapidly at different interfaces through the thickness, which greatly reduces the residual mechanical properties.

Table 1. Impact Data for Unstitched Plain Weave Laminates

Impact Energy J	Maximum Load (Kn)	Absorbed Energy J	Damage Area (mm^2)	Remarks
5	1.98	0.8	205	No visible damage
7.5	2.32	3.46	368	Dent, barely visible
10	2.5	2.49	586	Dent, barely visible
15	2.78	4.59	733	Dent, clearly visible
20	2.8	7.74	1074	Dent, clearly visible
25	2.85	14.9	1243	Dent, Backface split
30	2.79	17.8	1570	Dent, Partial penetration
35	2.8	22.7	2099	Dent, Partial penetration
40	2.8	16.4	3055	Full penetration

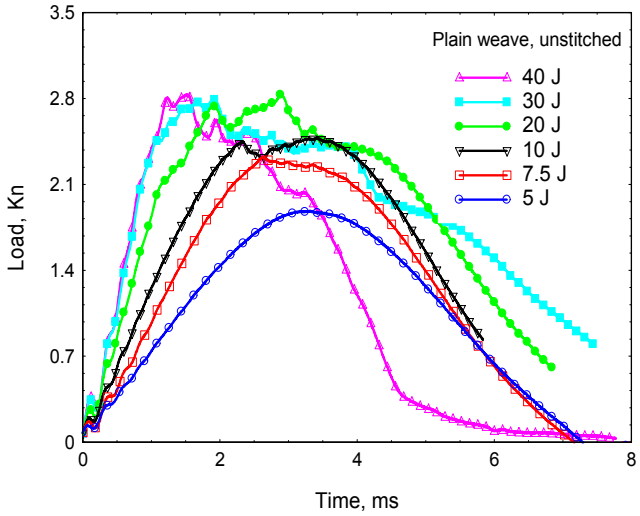

Figure 3. Load-Time Response for Unstitched Plain Weave Laminate Samples

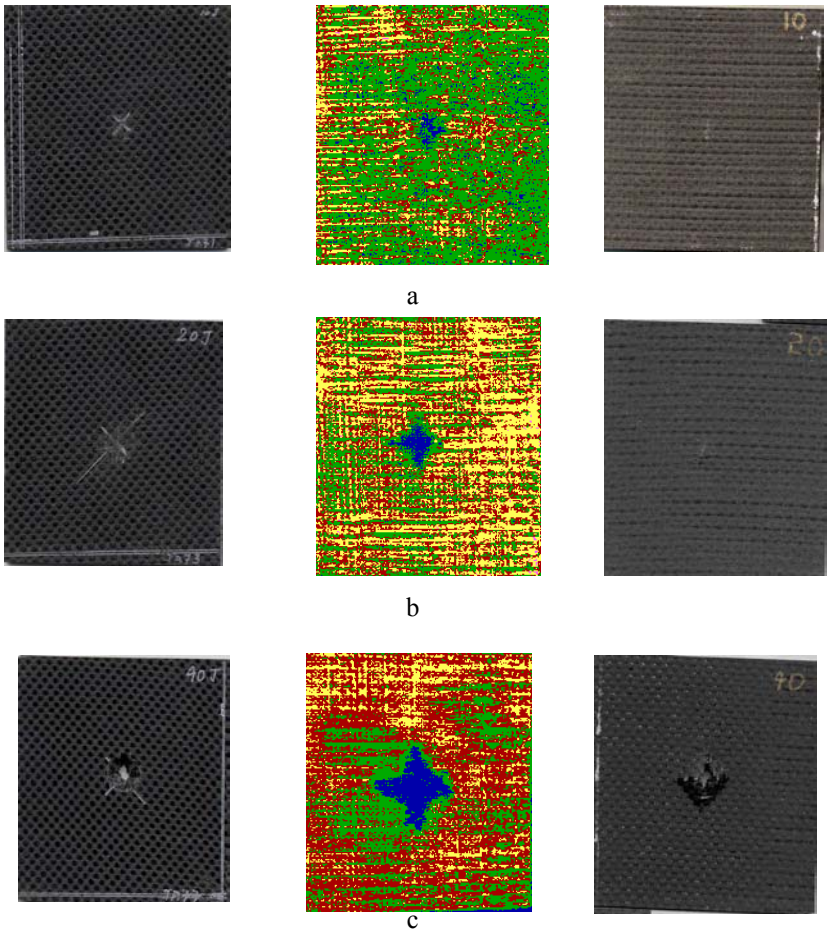

Figure 4. Front Side (left), Ultrasonic C-scan (middle) and Back Side (right) of Unstitched Plain Weave Laminates Impacted at a) 10 J, b) 20 J, and c) 40 J

Figure 5 exhibits the impact response plot and Figure 6 a-d (for energies 10, 20, 40, and 50 J respectively) illustrates front and back surface pictures with the ultrasonic c-scan images for 25.4-mm plain weave stitched carbon/epoxy laminates. Table 2 presents the summary of response in terms of peak load, absorbed energy, and damage area. In this case, the laminate seems to absorb a higher load as compared to unstitched laminates for a given impact energy. As can be seen from the table, there is no visible or ultrasonic indication of damage upto 10 J. The first sign of damage is seen at 15 J as a linear crack along the stitch line. This is true even at 20 J. At these two energy levels the damage is very little and all the energy (50 percent of impact energy) absorbed is taken up by the stitch line. At 25 J there is splitting damage along the stitch line, but the areal damage is again very small. Only at 30 J, there is visible dent at the impact point with splitting along stitch line at the back surface. The splitting along the stitch line is typical of stitched laminates, as the stitch locally damages the fabric, which gives away at impact energy in the range of 25–30 J. However, the overall effect on the laminate is the suppression of the damage due to stitching. At 35–50 J range of impact energy, the penetration of laminate takes place, with the damage being confined within the grid of the stitch line. With 25.4-mm stitch spacing, the damage is reduced by 1/3 as compared to unstitched laminate.

Table 2. Impact Data for 25.4-mm Stitched Plain Weave Laminates

Impact Energy (J)	Maximum Load (Kn)	Absorbed Energy (J)	Damage Area (mm^2)	Remarks
4.8	1.80	1.48	****	No visible damage
7.5	2.40	2.11	****	No visible damage
10	2.52	3.78	****	No visible damage
15	2.67	7.46	63	Backface crack
20	2.68	11.53	100	Backface crack
25	3.08	12.67	150	Dent, backface splitting
30	2.74	21.65	518	Dent, backface splitting
35	2.64	18.00	778	Partial penetration, backface split
40	2.82	17.35	1187	Penetration
45	2.90	24.70	1230	Penetration
50	2.90	21.94	2225	Penetration

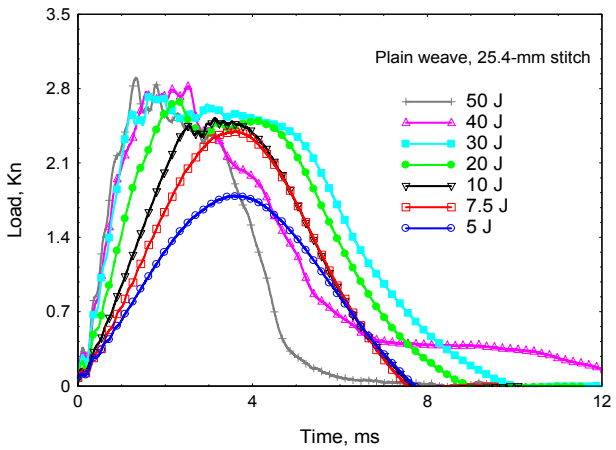

Figure 5. Load-Time Response for 25. 4-mm Stitched Plain Weave Laminate Samples

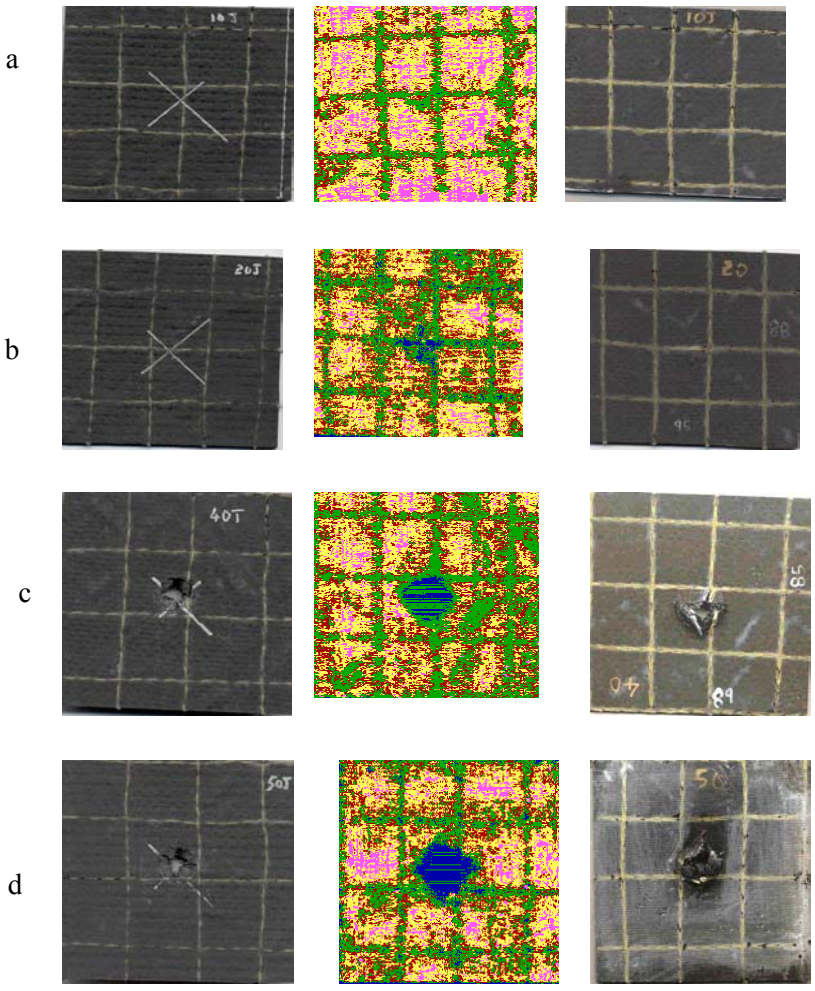

Figure 6. Front Side (left), Ultrasonic C-scan (middle), and Back Side (right) of 25.4-mm stitched Plain Weave Laminates Impacted at a) 10 J, b) 20 J, c) 40 J, and d) 50 J

Figure 7 indicates the impact response of 12.7-mm stitched laminates for energies ranging from 5–50J, while Figure 8 a-d illustrates the photographs of the front and back surfaces with the ultrasonic c-scan images of the samples impacted at 10, 20, 40, and 50 J respectively. Table 3 gives the summary of response in terms of peak load, absorbed energy, and damage area as obtained from the c-scan and the remarks based on the visual observations. In this case, the laminates sustain the impact till 15 J without any damage. It was seen both visually as well through ultrasonic evaluation that there was no damage in the sample. The first visible dent was observed at 20 J and the first sign of back surface splitting was observed at 25 J with the laminate absorbing more than 65 percent of energy through the stitches without apparently suffering major damage. At 40 J, there was partial penetration with the splitting along the stitch line and failure of the stitch. Full penetration occurred at 50 J with similar failure pattern on the back surface. Damage in 12.7-mm stitched laminate at 40J was about 1/2 and 1/6 the area as compared to 25.4-mm stitched and unstitched samples respectively. Further, the peak load for 12.7-mm stitched laminate saturates at about 3.65 Kn at 45 J as

compared to 2.8 Kn that an unstitched laminate can withstand. Thus, there is 30 percent increase in the load sustainability.

Table 3. Impact Data for 12.7-mm Stitched Plain Weave Laminates

Impact Energy (J)	Maximum Load (Kn)	Absorbed Energy (J)	Damage Area (mm^2)	Remarks
4.6	1.73	1.57	****	No visible damage
7.5	2.23	2.67	****	No visible damage
10.0	2.60	3.04	****	No visible damage
15	3.01	5.84	****	No visible damage
20	3.09	8.94	40	Dent
25	3.15	17.11	73	Dent, backface split
30	3.65	18.61	169	Dent, backface split
35	3.44	21.13	234	Dent, backface split
40	3.37	20.11	671	Partial penetration, backface split along stitch, thread breakage
45	3.65	29.80	932	Partial penetration, backface split along stitch, thread breakage
50	3.19	31.81	1620	Full penetration, backface split along stitch, thread breakage

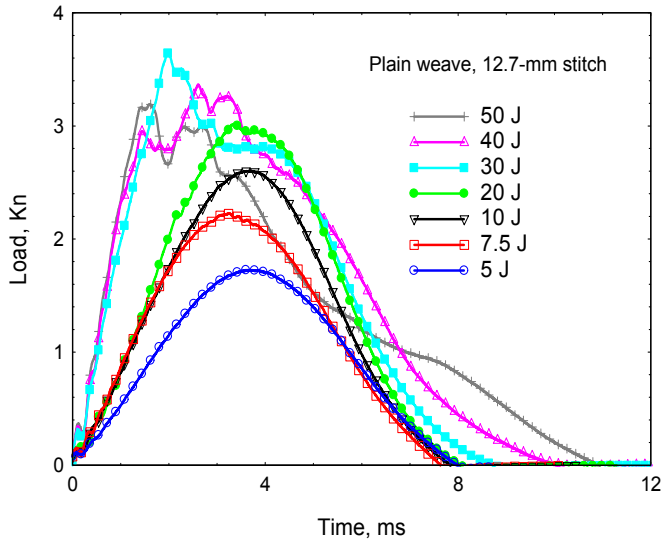

Figure 7. Load-Time Response for 12.7-mm Stitched Plain Weave Laminate Samples

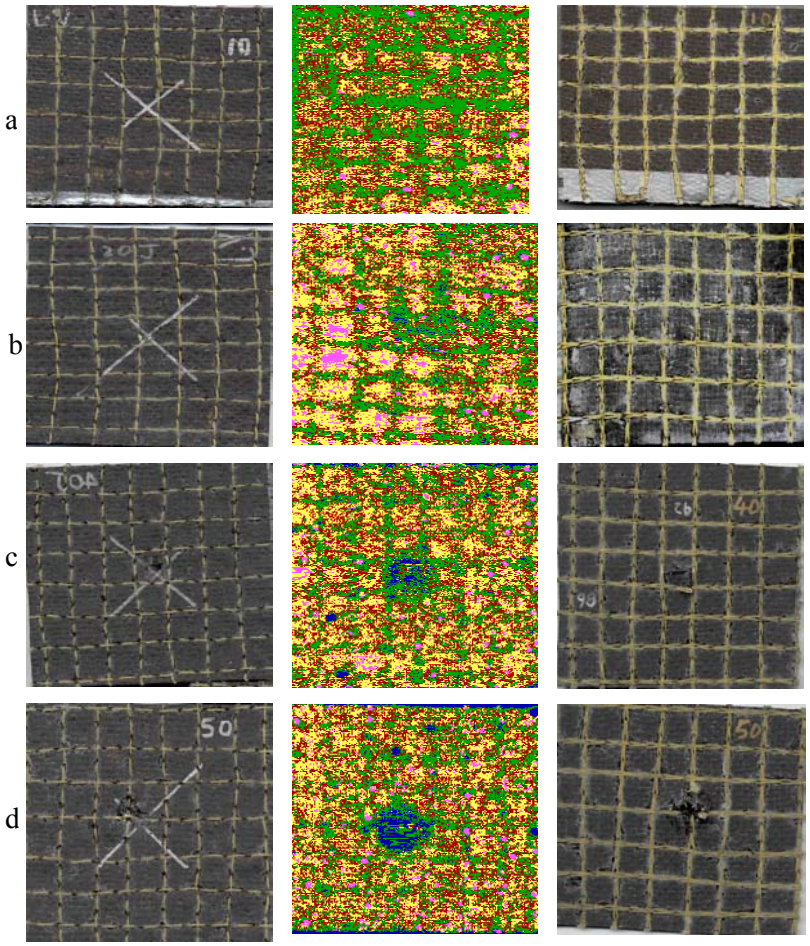

Figure 8. Front Side (left), Ultrasonic C-Scan (middle) and Back Side (right) of 12.7-mm Stitched Plain Weave Laminates Impacted at; a) 10 J, b) 20 J, c) 40 J, and d) 50 J

A comparison of the response of three types of laminates discussed in this study is best illustrated by plotting the damage area in a single graph as shown in Figure 9. In this graph the damage area is plotted as a function of impact energy for unstitched, 25.4-mm stitched, and 12.7-mm stitched laminates. It is clearly evident from this plot that there is considerable advantage to be gained from stitching. Stitching restricts the size of the damage, as a large amount of energy has to be expended in overcoming the resistance offered by the stitches. Once the damage due to impact is reduced, then the residual properties are relatively improved over the unstitched laminates, thereby enhancing the scope of increasing design allowables. The size of the post-impact repair, if warranted, will be considerably reduced, thereby reducing the overall cost.

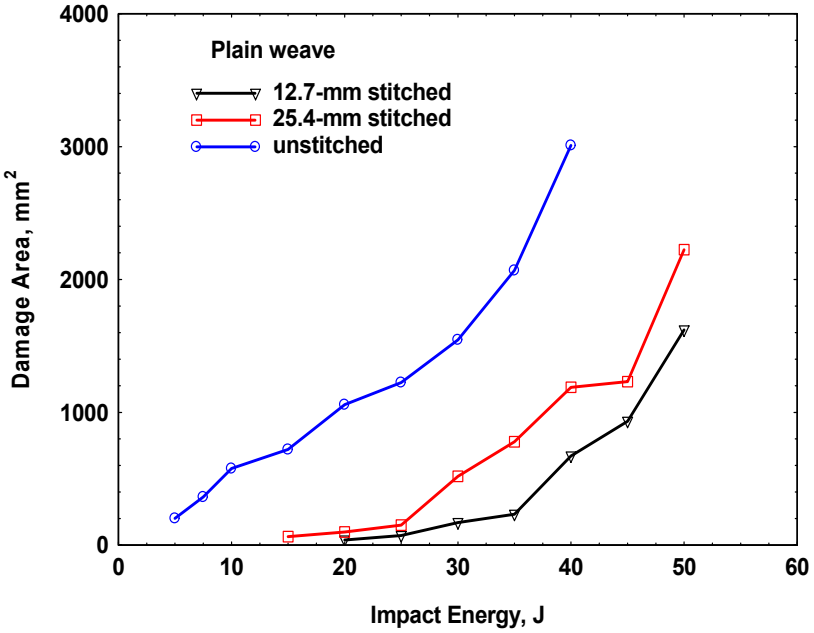

Figure 9. Damage Area Versus Impact Energy for Unstitched, 25.4-mm Stitched and 12.7-mm Stitched Plain Weave Carbon/Epoxy Laminates

1.3.2 Satin Weave Carbon/Epoxy Composite

Figure 10 illustrates the impact response of unstitched satin weave laminates. Figure 11 a-d give front and back surface pictures along with ultrasonic c-scan images of the samples impacted at 10, 20, 40, and 50 J, respectively. The impact parameters along with the remarks and projected damage area as measured from ultrasonic c-scan images are given in Table 4. From the transient response curves illustrated in Figure 10, it is seen that the peak load increases with an increase in impact energy, and also the time to peak load decreases, which is a common feature of the impact loading on laminated composites. The curves for 5, 7.5, and 10 J show symmetric loading-unloading response with no apparent oscillations in the load. This indicates that the laminate is able to sustain the impact loading without any damage. Ultrasonic evaluation of the samples after the test, confirm these observations. Further, there was no visible indication of any dent or damage either at the point of impact and the back surface of the laminate. The first visible dent was seen at 20 J, which is well illustrated from the transient response also by means of few oscillations in the load. From 20–30 J, there is gradual increase in the dent size at the point of impact. At 20 and 25 J, 40 percent of the energy is absorbed by the samples in terms of creation of a dent. At 30 J, a dent becomes clearly visible. A partial penetration is observed first at 35 J with back surface cracking along the interfaces between the fibers resulting in sudden increase in the damage area. About 2/3 of the impact energy is absorbed in the process, with an increase of three and half times damage area as compared to that observed for 20-30 J energies. Damage area, dent depth and crack lengths increase further at 40 and 45 J. The maximum peak load for satin weave laminate is 3.75 Kn, which is about 0.95 Kn more than that sustained by plain weave unstitched laminate. However, the complete penetration of the sample takes place at 50 J with

the back surface splitting. Here again, the damage is very much confined to the region around the impact area.

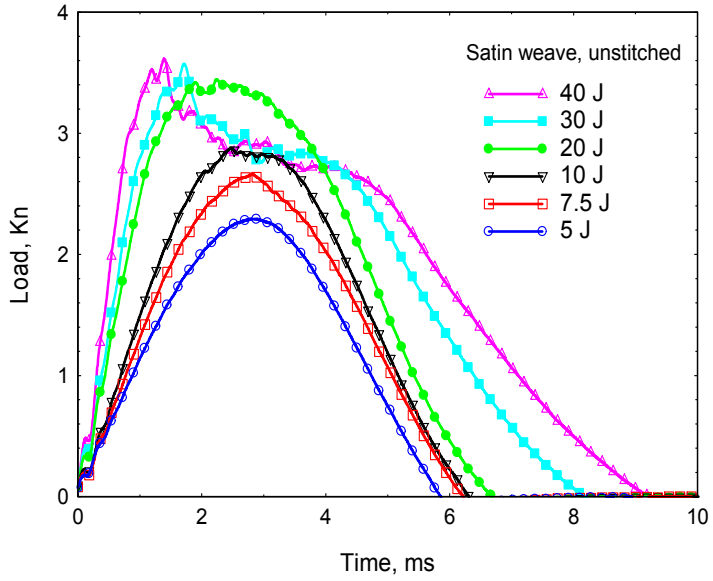

Figure 10. Load-Time Response for Unstitched Satin Weave Laminate Samples

Table 4. Impact Data for Unstitched Satin Weave Laminates

Impact Energy, J	Maximum Load, Kn	Absorbed Energy, J	Damage Area mm^2	Remarks
5	2.29	1.36	-	No damage
7.5	2.67	2.4	-	No damage
10	2.88	4.01	-	No damage
15	3.51	5.33	-	Barely visible dent at the point of impact
20	3.45	8.82	340	Dent at point of impact, tiny crack on back surface
25	3.5	9.62	403	Dent at impact point, back surface orthogonal cracks
30	3.57	18.47	453	Dent at impact point, protrusion and cracking on the back surface
35	3.69	22.36	1413	Dent at impact point, protrusion and cracking on the back surface
40	3.62	27.85	1972	Indentation at impact location, cracking and fiber two breakage at back surface
45	3.75	32.26	2479	Partial penetration, splitting of back surface
50	3.59	35.98	3208	Deep penetration, splitting of back surface

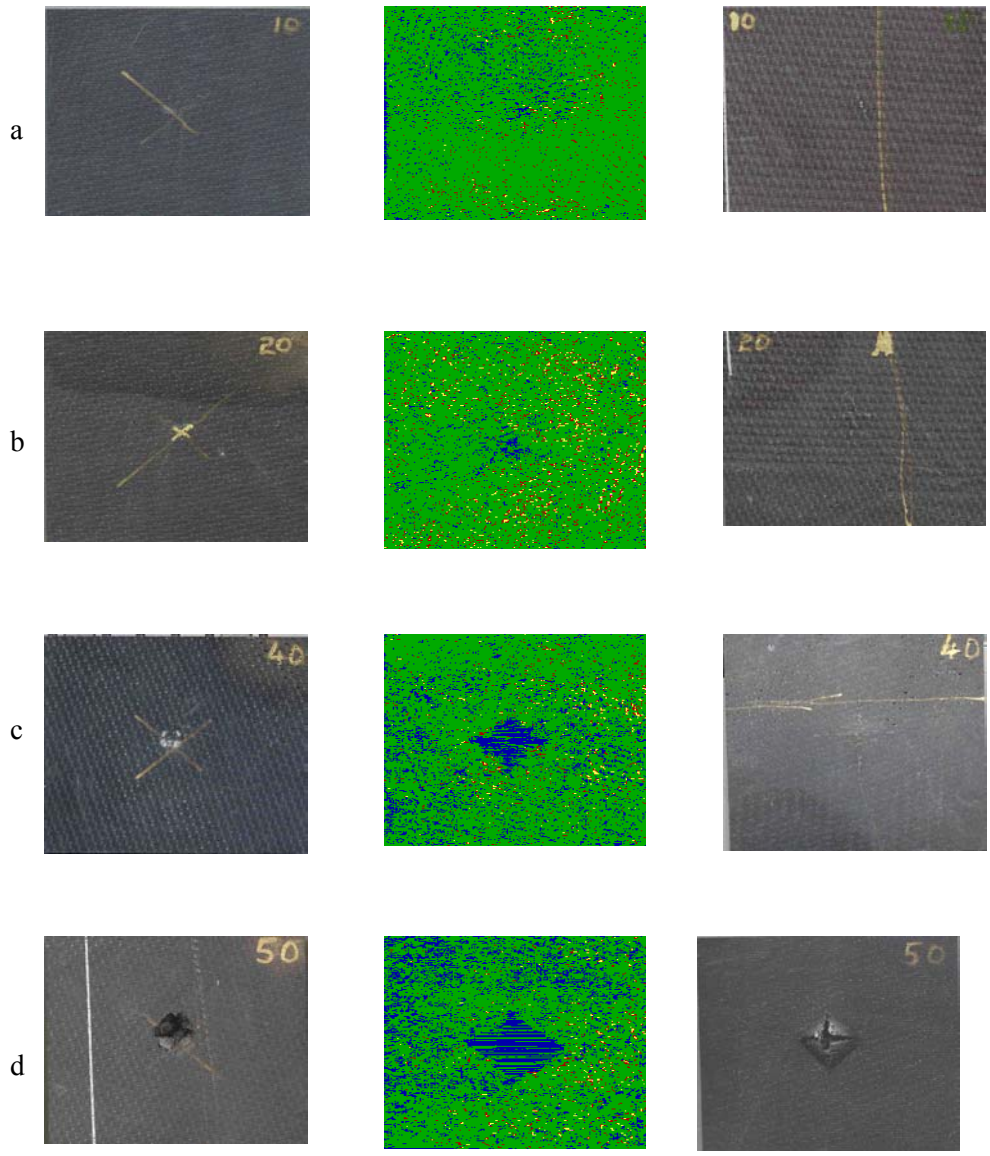

Figure 11. Front Side (left), Ultrasonic C-scan (middle) and Back Side (right) of Unstitched Satin Weave Laminates Impacted at; a) 10 J, b) 20 J, c) 40 J, and d) 50 J

Figure 12 illustrates the impact response of 25.4-mm stitched satin weave laminates. Figures 13 a-d give front and back surface pictures along with ultrasonic c-scan images of the samples impacted at 10, 20, 40, and 50 J respectively. The impact parameters along with the remarks and projected damage area as measured from ultrasonic c-scan images are given in Table 5. The curves for 5, 7.5, and 10 J show symmetric loading-unloading response with no apparent oscillations in the load. This indicates that the laminate is able to sustain the impact loading without any damage. The first visible dent was evident at 20J, which is well illustrated from the transient response by means of few oscillations in the load. However, no damage was discernable from ultrasonic c-scan data. From 20–30 J, there is gradual increase in the dent size at the point of impact. Between 25– 35J of impact, there was visible dent at the impact point with cracking at the back surface. About 60 percent of the impact energy is absorbed by the laminate in creating the damage. A partial penetration is observed first at 40 J

with the splitting of back surface along the stitch line and breakage of thread. About 2/3 of the impact energy is absorbed in the process. At 45 J, there is sudden increase in the damage size (three and half times as compared to 40 J sample) with increasing penetration. Damage area, dent depth and crack lengths increase further at 40 and 45 J. There is complete penetration of the sample at 50 J. Further, all the damage is confined within the grid. The maximum peak load in the case of 25.4-mm stitched satin weave laminate is 4.04 Kn, which was sustained at 30 J. Hence, 25.4-mm stitched laminate sustain 0.29 Kn more load than unstitched laminate.

Table 5. Impact Data for 25.4-mm Stitched Satin Weave Laminates

Impact Energy, J	Maximum Load, Kn	Absorbed Energy, J	Damage Area mm^2	Remarks
5	2.04	1.52	-	No Visible Damage
7.5	2.57	2.19	-	No Visible Damage
10	2.68	4.82	-	No Visible Damage
15	3.34	4.58	-	No Visible Damage
20	3.32	7.94	-	Dent
25	3.31	14.64	48	Dent, backface split
30	4.04	17.97	106	Dent, backface split
35	4.01	19.54	248	Dent, backface split
40	3.67	25.19	434	Partial penetration, backface split along stitch, thread breakage
45	3.71	30.39	1393	Partial penetration, backface split along stitch, thread breakage
50	3.46	21.80	1946	Full penetration, backface split along stitch, thread breakage

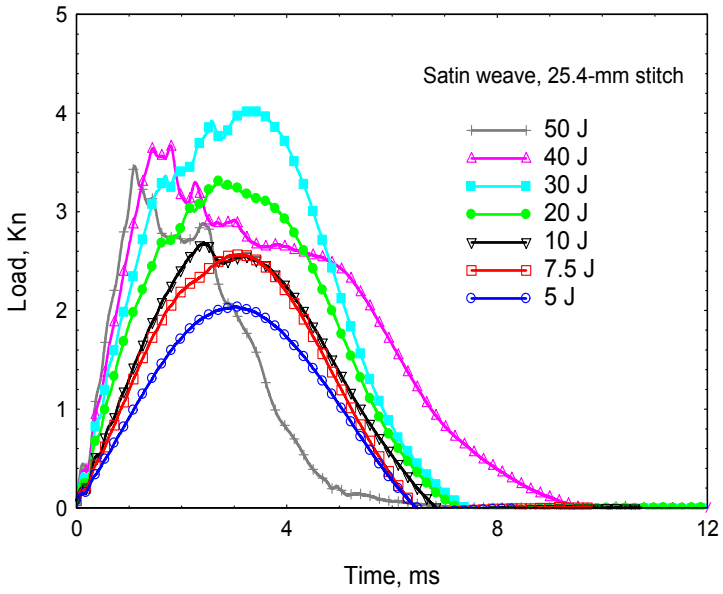

Figure 12. Load-Time Response of 25.4-mm Stitched Satin Weave Carbon/Epoxy Laminates

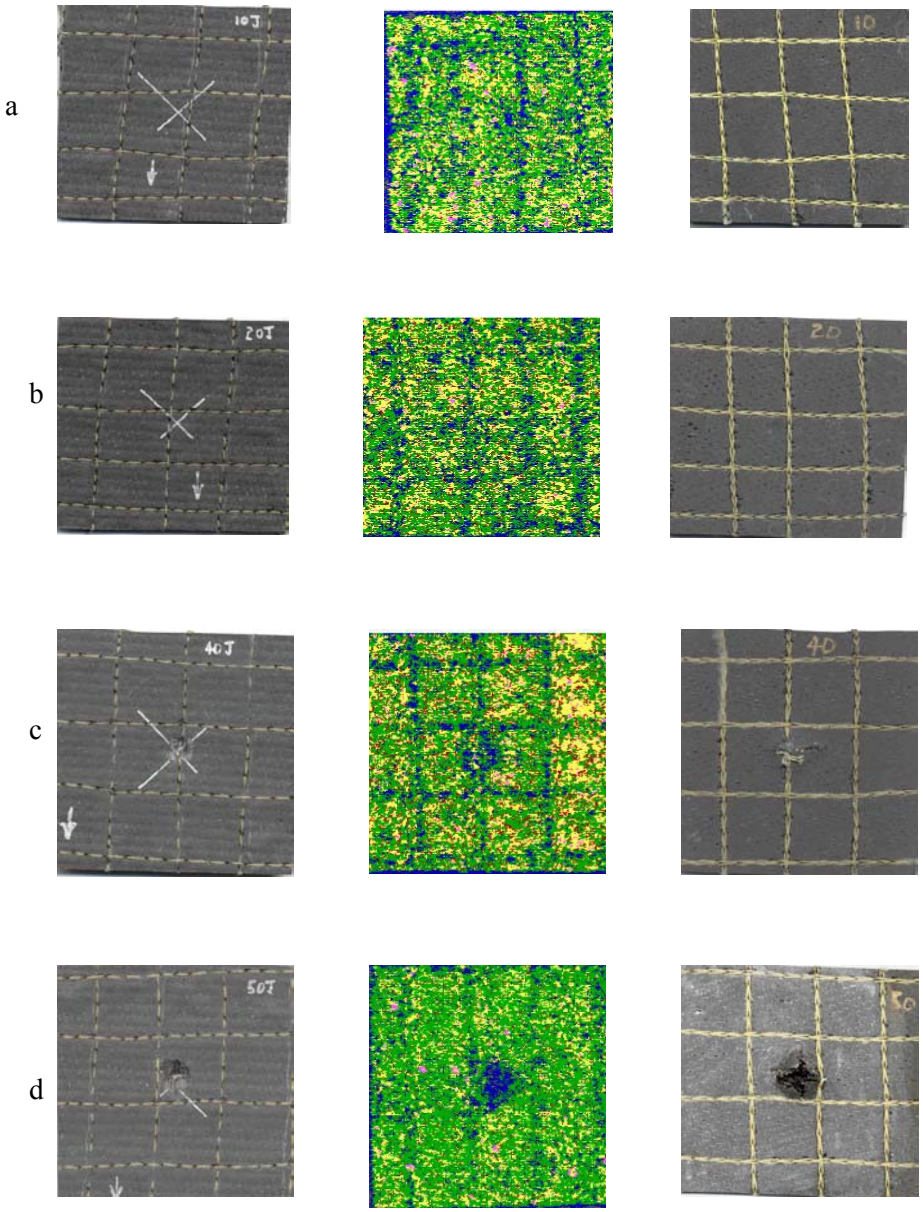

Figure 13. Front Side (left), Ultrasonic C-scan (middle) and Back Side (right) of 25.4-mm Stitched Plain Weave Laminates Impacted at; a) 10 J, b) 20 J, c) 40 J, and d) 50 J

Figure 14 illustrates the impact response of 12.7-mm stitched satin weave laminates. Figure 15 a-d gives front and back surface pictures along with ultrasonic c-scan images of the samples impacted at 10, 20, 40, and 50 J, respectively. The impact parameters along with the remarks and projected damage area as measured from ultrasonic c-scan images are given in Table 6. From the transient response curves illustrated in Figure 14, it is seen that the peak load increases with increase in impact energy and also the time to peak load also decreases. The curves for 5, 7.5, and 10 J show symmetric loading-unloading response, indicating no damage in the laminate. The laminate in undergoing elastic deformation absorbs all the

energy. For the sample impacted at 20 J, there is small change in the slope of the curve at 3.0 Kn load. However, neither visible indications nor ultrasonic studies revealed any damage. First, quantitative damage was observed through ultrasonic evaluation at 25 J. The first visible indication of damage was seen at 30 J through backface splitting along the stitch line. Since the back surface gave away, there was a sudden drop in the peak load. However, there was a redistribution of load, as evident from the increasing load in the transient response curve. Since the damage was through linear splitting, the size of the damage was very much confined to the location along the stitch line. Even though there was increased energy absorption of about 50 percent, at 30- 45 J, the damage was again very much confined along the stitch line within the grid where the impactor hits the laminate. This was again reflected in the limited damage sizes. At 50 J, there was a partial penetration of the laminate with back surface splitting and breakage of thread. However, when compared to unstitched and 25.4-mm stitched laminates, it was seen that the damage size was considerably reduced.

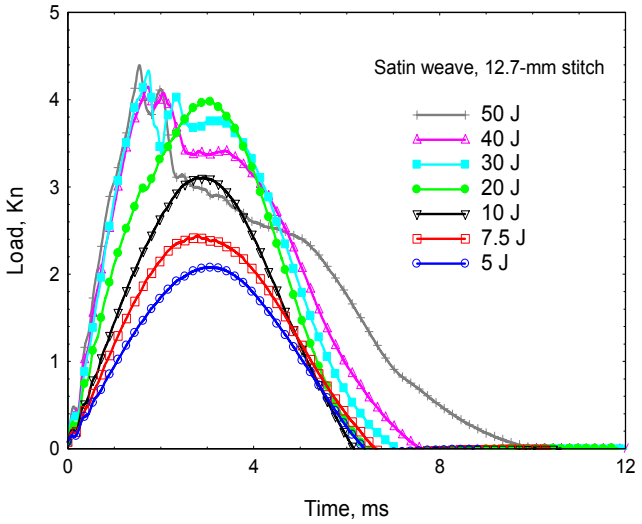

Figure 14. Load-Time Response of 25.4-mm Stitched Satin Weave Carbon/Epoxy Laminates

Table 6. Impact Data for 12.7-mm Stitched Satin Weave Laminates

Impact Energy (J)	Maximum Load (Kn)	Absorbed Energy (J)	Damage Area (mm^2)	Remarks
5	2.08	1.51	-	No visible damage
7.5	2.44	2.84	-	No visible damage
10	2.74	2.85	-	No visible damage
15	3.11	3.28	-	No visible damage
20	3.64	4.57	-	No visible damage
25	3.98	5.42	34	No visible damage
30	3.79	6.69	78	Backface split along stitch line
35	4.33	17.94	92	Dent, backface split along stitch line
40	4.15	21.55	187	Dent, backface split along stitch line
45	4.28	25.67	280	Dent, backface split along stitch line
50	3.74	32.92	1126	Partial penetration, backface split along stitch, thread breakage

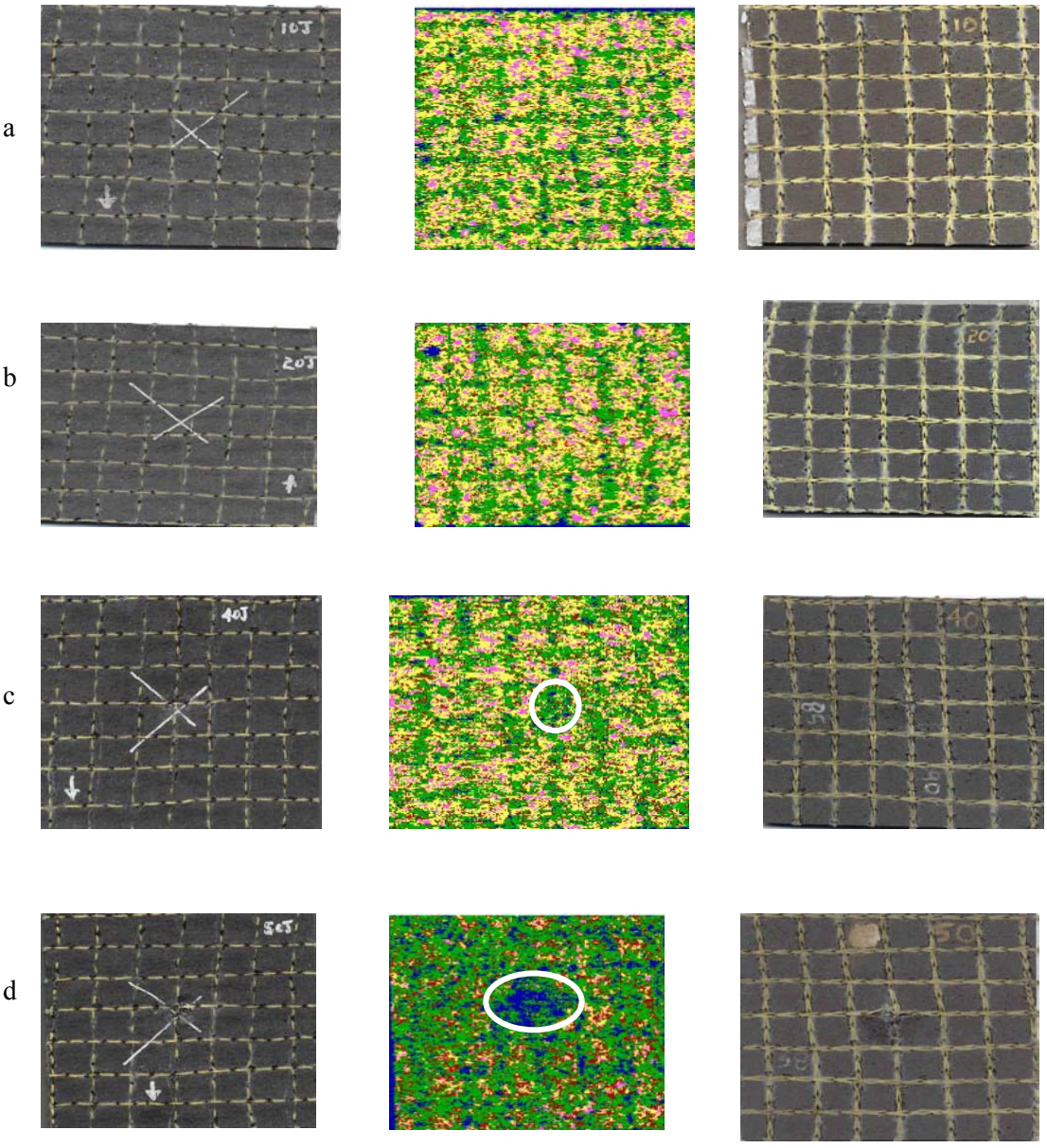

Figure 15. Front Side (left), Ultrasonic C-scan (middle), and Back Side (right) of 25.4-mm Stitched Plain Weave Laminates Impacted at; a) 10 J, b) 20 J, c) 40 J, and d) 50 J

Figure 16 illustrates the variation of projected damage area as determined through ultrasonic c-scan evaluation with impact energy for satin weave carbon/epoxy laminates. From this plot, it is again demonstrated that there is a considerable reduction in the impact damage area for stitched laminates. The closer the stitch spacing, the better the impact resistance and increased damage tolerance. Satin weave laminates exhibit better impact response as

compared to plain weave laminates. This is attributed to the fabric architecture. In the plain weave fabric, the fiber tow in the warp direction crosses over every other fiber tow in the fill direction, as shown in the schematic diagram in Figure 17. The angle made over the crossing, which is called crimp angle, is thus steep and is repeated for each tow in both fill and warp direction. Hence, there is a considerable reduction in the in-plane properties of the laminate made using plain weave architecture. In comparison, in eight-harness satin weave fabric, the fiber tow in the warp direction runs over seven fiber tows in the fill direction before crossing under the eighth tow in the fill direction, as shown schematically in Figure 18. This pattern in repeated over the entire width of the fabric. This will result in much straighter architecture without any apparent indication of the weave. The resulting laminate will be very close to unidirectional laminate, with much higher in-plane properties as compared to plain weave fabrics. Under impact loading, the tensile failure initiates through in-plane failure of the bottommost ply. The fabric with better in-plane properties would naturally sustain higher stresses, which in the current case is satin weave. Further, the failure initiation is more likely though tensile failure of the fiber tows. In the case of plain weave fabric, the failure initiation is more likely to be through shear fracture of the fiber tow.

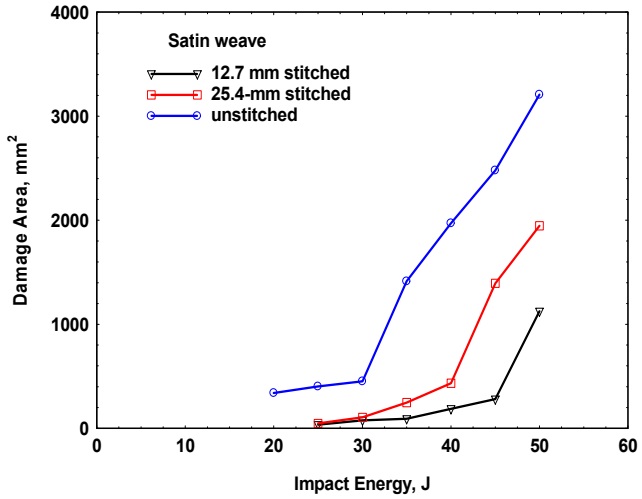

Figure 16. Damage Area Versus Impact Energy for Unstitched, 25.4-mm Stitched and 12.7-mm Stitched Satin Weave Carbon/Epoxy

1.4 Conclusions

Investigations were carried out to study the response of woven fabric laminates manufactured by an affordable liquid molding process, VARIM, under simulated low-velocity impact loading conditions. Both stitched and unstitched laminates were considered. For stitching, three-cord Kevlar thread was employed and the dry fabric stack was stitched in a lockstitch pattern with a stitch pitch of 6-mm orthogonal grid pattern with 25.4 and 12.7-mm grid spacing. Laminates were impacted at energies ranging from 5–50 J. Unstitched plain weave laminates could sustain energy upto 40 J before the impactor penetrated the laminates. Whereas stitched laminates withstood impact energy up to 50 J before being perforated. The stitching increased the maximum load taken by the laminate and also reduced the damage size within the grid of the stitch. Damage size was reduced by 1/3 for 25.4-mm stitched and by 1/6 for 12.7-mm stitched laminates as compared to the unstitched laminates. Transient

response of the woven fabric laminates showed no steep drop in the load at higher energy, as is normally observed in unidirectional laminate. There was a conspicuous absence of extended delamination damage in woven fabric composites. The weave pattern prevents the back surface from splitting, thereby preventing the onset and propagation of delamination damage. The predominant damage mode is indentation and penetration, which is limited to the area surrounding the point of impact. Hence, there is a potential improvement is the damage tolerance in the eventuality of impact damage during service. In addition, due to the lesser damage, repair costs will be lower.

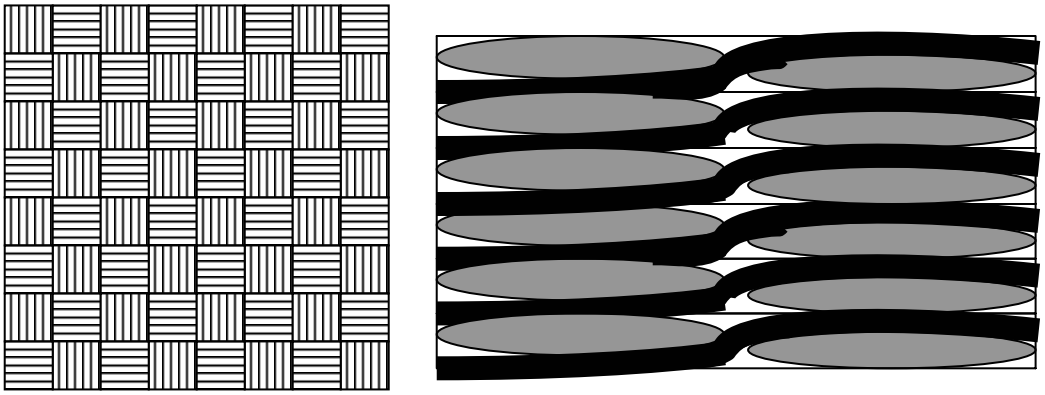

a)

b)

Figure 17. Plain Weave Fabric; a) Planform, and b) Section

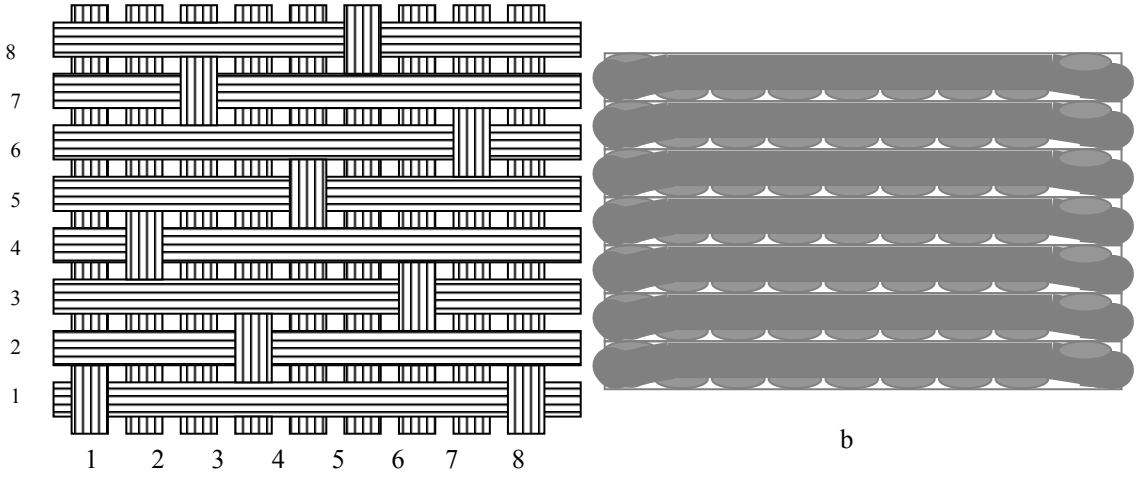

a

b

Figure 18. Schematic of Eight-Harness Satin Weave Fabric Laminates; a) Planform and b) Section

There are considerable advantages to be gained in having woven fabric composite laminates over unidirectional laminates, when the design considerations are affordability and survivability. Though in-plane properties of woven fabric composites are known to be lower

compared to unidirectional laminates, they have excellent impact properties. Using, low-cost processing methods like VARI, the cost of producing structural composite parts can be drastically reduced. Further, the dry fabric can be stitched to improve the damage resistance. This would facilitate the fabrication of components with increased damage tolerance.

2.0 Low-Velocity Impact Testing and Post Impact Characterization of Woven Fabric Composites

Woven textile composites are replacing multidirectional laminates primarily because of their properties in mutually orthogonal directions as well as more balanced properties and better impact resistance. One of the affordable low-cost woven composites is manufactured by using graphite fibers and SC-15 epoxy resin through resin infusion or resin transfer molding processes. Before these composites can be used in aircraft as primary load carrying structures, it is essential to investigate the behavior of these laminates when subjected to low velocity impact loading.

This research addresses the progressive damage and deformation mechanics of thin and thick woven composites subjected to low-velocity impact loading. The plain woven carbon fabric is used in conjunction with two different resin systems–SC-15 epoxy resin and Derakane 510A-40 vinyl ester resin. It has been proved that SC-15 epoxy resin has a very good resistance to fracture by ballistic impact. Derakane 510A-40 is an inexpensive resin and designed to offer a maximum degree of fire retardance combined with enhanced chemical resistance and toughness. In addition, the impact performance of these two resin systems is compared in addition to the size effect study. The impacted specimens are tested in compression to study the stiffness reduction. Also, the impacted specimens are tested in tension-tension fatigue, followed by static tension tests. These tension tests are performed to evaluate the stiffness reduction as a function of post impacted fatigue loading.

2.1 Introduction

Composite materials have advantages over traditional materials in high specific strength and high specific stiffness. This is the main reason that composite materials are continuously replacing traditional materials despite their inherent shortcomings in other characteristics. Multidirectional laminates are generally preferred in structural applications. Angles of the individual lamina and their stacking sequence in the laminate plate are designed according to the intended loading and geometry of the structure. However, these laminates could be very weak for unintentional loading, especially for the out-of-plane impact. In these circumstances, various alternative composite materials like textile composites are being developed and tried in place of conventional multidirectional laminates, principally because of their good properties in mutually orthogonal directions as well as more balanced properties and better impact resistance.

2.2 Review of Earlier Work

Most of the literature on the woven composites is related to predict the elastic and static strength properties. Earlier works were based on modified laminate theory by Ishikawa and Chou [34, 35]. Later analytical models accounting undulation both the fibers were proposed by Naik and Ganesh [36]. Three dimensional finite element models are also constructed by Whitcomb [37] and study of progressive failure and strength by Whitcomb and Srirengan [38].

Impact studies on woven composites used in aircraft applications are important for obvious reasons. There are very few references related to the study of low-velocity impact on woven composites. Most of the past studies are related to the ballistic impact. Espinosa et al. [39] developed a technique to simultaneously record projectile velocity histories that target back surface out-of-plane motion. They observed the failure mechanisms and showed that there are three regions with different failure mechanisms in the S-2 glass woven composites. Navarro [40-41] conducted experimental and analytical ballistic studies on woven E-glass/epoxy composite laminates. Navarro found proportionality relations of initial impact energy and absorbed energy. For example, with initial impact energy above the ballistic limit, the absorbed energy remained approximately constant regardless of the increase of the initial striking velocity of the projectile.

Kang et al. [16] conducted studies showing how different composites stitched at different densities improved mechanical and impact properties. Wu [29] conducted progressive studies on E-glass/epoxy woven composites. However, Wu's progressive study involved ranging the impact velocities from low to ballistic speeds and energies.

Mahfuz et al. [42] conducted low-velocity impact studies on woven composite encompassing three material systems investigating the failure modes and mechanisms. This damage tolerance study included experimental and numerical analysis. The damage in this study was assessed through ultrasonic measurements and scanning electron micrographs. Walsh et al. [33] conducted studies to examine the deformation and penetration failure mechanisms of plain weave Spectra polyethylene fiber with vinyl ester and polyurethane resin matrix composites. The literature review indicates that very little work is reported related to progressive deformation and damage mechanics of woven composites subjected to low-velocity impact loading. Furthermore, the degradation of stiffness in post impacted laminates is not studied and needs further investigation. Hence the specific objectives of the proposed research are presented in the following section.

2.3 Objectives

- To study the progressive deformation and damage mechanics of woven composite subjected to low-velocity impact loading.
- To study the scaling (size) effects on the low velocity impact behavior of woven composites.
- To study the degradation in stiffness of post impacted woven composites subjected to static compressive loading.
- To study the degradation in stiffness of post impacted woven composites subjected to tension-tension fatigue loading.

2.4 Material Systems

- Plain woven carbon fabric (8, 16, and 24 layers) and SC-15 epoxy resin.
- Plain woven carbon fabric (8, 16, and 24 layers) and 510A vinyl ester resin.

Three different thicknesses covering thin composites to thick composites are being investigated. The composite panels were fabricated using a vacuum-assisted resin transfer molding (VARTM) method. In this process, a mold is loaded with the reinforcement material and then it is closed. The resin is injected into it. The mold with the preform is often put under vacuum so that the vacuum removes all of the entrapped air in the preform and speeds up the resin transfer molding RTM process. Typically, the resin is injected at the center of the top surface of the mold and the flow of resin occurs radially outward till it reaches the vent lines. In this process, the flow of the resin occurs in the plane as well as in the transverse direction of the preform. The fiber architecture, permeability of the preform, and the fabric crimps have an influence on the wetting of the fabric. It has been found that the moduli and ultimate tensile strength of RTM and VARTM panels are comparable if the volume of the fibers is the same. The fatigue performance depends on the resin content, and with the same amount of resin, the performance was comparable for both the above RTM and VARTM methods.

2.4.1 SC-15 Epoxy Resin

The resin used in the fabrication of the composite panel was SC-15 epoxy resin. It has been proved that this resin has a very good resistance to fracture by ballistic impact. The details of the properties of this resin are provided in Table 7. Some tests have been conducted to find out the properties of this resin and to lay down some of the parameters like curing time, pot life, viscosity versus the temperature response, and specific gravity of the resin.

The viscosity of the resin is measured with the help of a viscometer to know the viscosity of the mixture of the resin and the hardener. The viscometer is first calibrated to show accurate readings of viscosity. The calibration is done using three calibrating liquids. The correction factors are applied to the viscosity measurements to get the exact readings.

Table 7. Properties of SC-15 Epoxy Resin

Property	**Value**
Viscosity at ambient temperature, cps	350
Specific gravity	1.1
T_g Dry °F	237
T_g Wet °F	180
Tensile modulus, Msi	0.49
Flexural strength, Ksi	19.1
Cost $ per lb	7

The viscometer is manufactured by Lab Line Instruments Inc. The viscometer operates on the principle of rotating a cylinder or disc immersed in the material under test and measuring the torque necessary to overcome the viscous resistance to rotation. The disc rotates at a known speed and the speed is decided based on the approximate viscosity of the resin and size of the disc.

Specifications of Viscometer:

1. Accuracy: +/- 1.0 percent of the full scale in use.
2. Resolution: +/- 0.1 percent of the full scale in use.
3. Repeatability: +/- 0.2 percent of the full scale in use.
4. Ambient Temperature: +10 °C to +40 °C.
5. Resolution: 0.01 to 1000 cP.
6. Humidity: 5 to 95 percent RH non-condensing.
7. Model Number: 4537.

The viscometer was used with the spindle number L2 and with a rotating speed of 30 rpm. The experimental set-up for the viscosity measurement test is shown in the Figure 19. First, the viscosity of resin versus the temperature was measured, so that the viscosity of mixture of resin and hardener could be determined while fabricating the composite panel. Consideration of this data, determines whether heat is to be applied to the mold while fabricating the panel or whether the process will be done at room temperature. Figure 20 gives the graph of viscosity versus time.

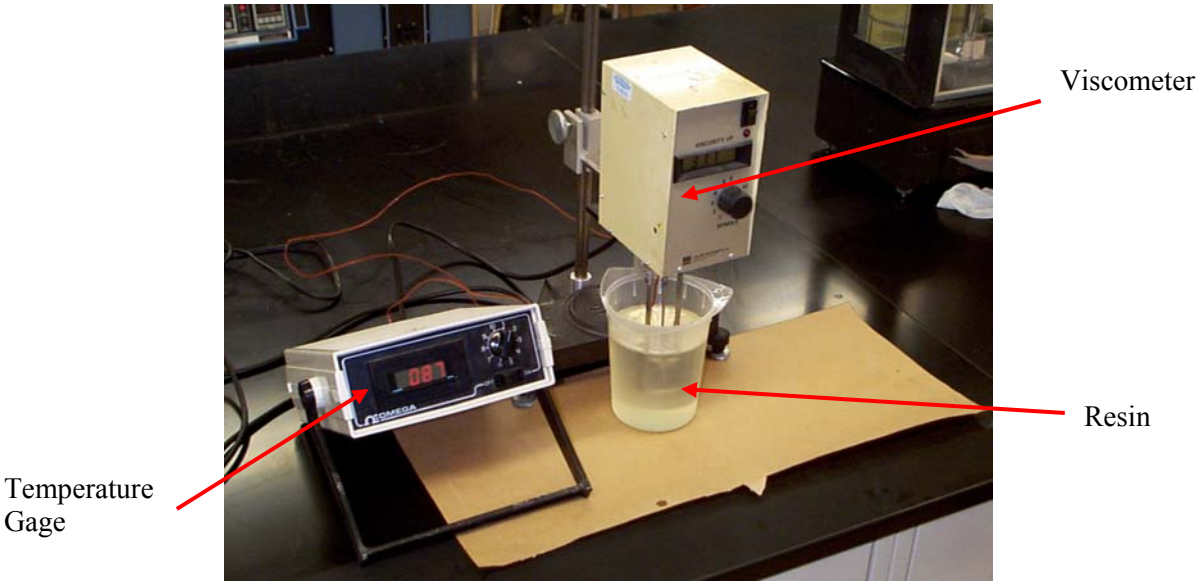

Figure 19. Arrangement for Measuring the Viscosity of SC-15 Resin

After finding the viscosity at which the resin is to be injected into the mold, it is helpful to know whether the reaction of resin and hardener is exothermic or not. The temperature versus time response (Figure 21) is measured to know the maximum temperature attained by the resin mixture during the gelling process. The components used in the mold should have a melting temperature above the maximum temperature reached during the curing process. Figure 19 gives a general idea of the temperature-versus-time response. The viscometer was calibrated with the help of three calibrating fluids for three different ranges of viscosities, and a correction factor is to be applied to the readings of the viscometer. The correction factor is shown in Equation 1:

Correction Factor = 1.567 * (Viscosity Reading) $^{-0.0519}$
Actual Viscosity = Correction factor * Viscometer Reading (1)

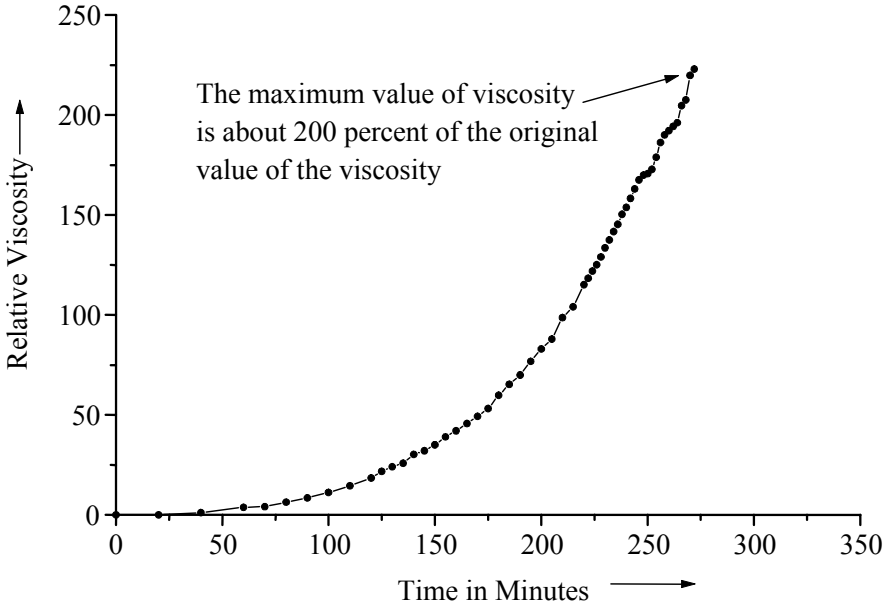

Figure 20. Relative Viscosity Versus Time for SC-15 Resin Mixture

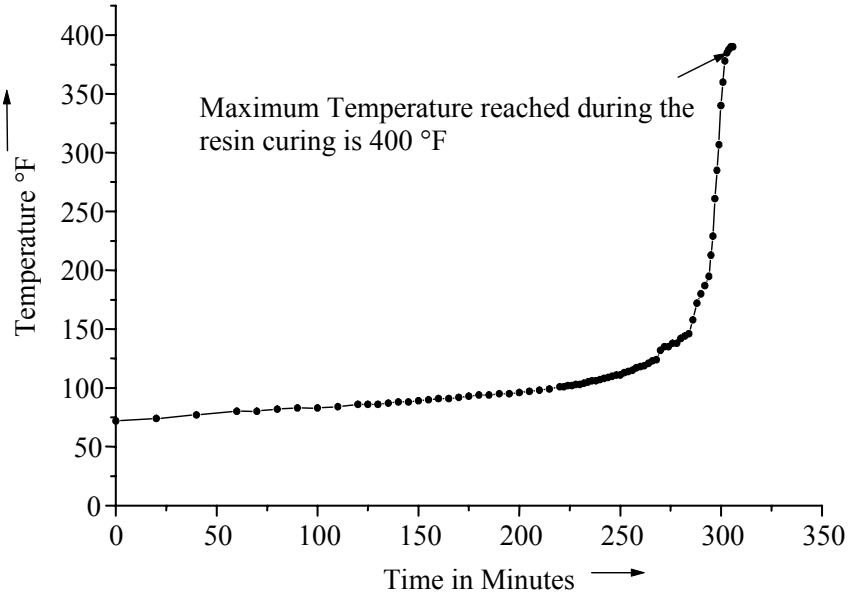

Figure 21. Temperature Versus Time Response for SC-15 Resin Mixture

2.4.2 Derakane 510 A-40 Vinyl Ester Resin

Derakane 510A-40 resin is manufactured by Dow Chemical Company, Inc. This vinyl ester resin is a brominated bisphenol-A; based vinyl ester designed to offer maximum degree of fire retardance combined with enhanced chemical resistance and toughness. Viscosity of this resin is 350 cps at ambient temperature 77 °F, which is most suitable for the VARTM process. The important properties of this resin are tabulated in Table 8:

Table 8. Properties of Derakane 510A-40 Vinyl Ester Resin

Property	Value
Viscosity at ambient temperature, cps	350
Specific gravity	1.23
Heat distortion temperature at 264 psi applied stress, °F	225
Tensile strength, Ksi	10.5
Tensile modulus, Msi	0.5
Flexural strength, Ksi	18
Flexural modulus, Msi	0.53
Cost $ per lb	1

Viscosity study has not been conducted in house on this resin. However, gel time studies have been performed to determine the best mixing combination to deliver the maximum gel time. Gel time is the amount of time that occurs between mixing of the chemicals and hardening of the resin. A gel time of approximately 2 hours was found. This allows time enough to flow a panel size of approximately 3 by 4 feet with an extra 30 minutes of breathing room.

2.5 VARTM

In the current work, the VARTM process is used to fabricate the laminates. Aluminum plate was used for the fabrication. For thick woven composites, two layers of Frekote-700 NC are applied to the mold surface. A coating of sand paste wax is also applied to the surface for easy release of the composite panel. This is a precaution in addition to the Frekote being applied. A release fabric, which is a porous release material, was used at the bottom. This leaves an impression on the part suitable for secondary adhesive bonding (like tabbing) without further surface preparation. Plain weave fabric is placed in a room with controlled temperature and dry atmospheric conditions. This prevents the contamination of the fabric from water condensation. The fabric is cut to the required dimensions and then stacked one on top of another. A precaution to be taken in stacking is keeping the fill and the warp fibers perpendicular to each other and parallel to the corresponding fill and warp fibers of the other plies. Eight, sixteen, and twenty-four layers of the fabric are laid in the above fashion in the middle of the enclosure provided by the sealant and on top of the peel ply. A release fabric is placed on top of the layup. This is a porous release material which facilitates the resin flow through and leaves an impression on the part suitable for secondary bonding without further surface preparation. A release fabric is placed as a distribution medium over the top of the setup. The distribution medium is NALTEX mesh laid on top of the top release fabric. This helps to maintain an even distribution of resin on the top of the panel and also facilitates the flow of resin through the thickness of the panel. Spirally cut tubes are then placed as resin and vacuum distribution lines. These lines are laid above the distribution media at two sides

of the fabric layup and go along the length. The resin line is closed at one end and connected to resin supply through the peristaltic pump at the other end. The vacuum line is closed at one end and connected to vacuum pump through the vacuum gage. It is standard practice to place the closed ends of these lines opposite to each other. A breather layer is placed over the resin distribution media, resin and vacuum lines. It also acts as a buffer between the vacuum bag wrinkles and part surface. It is a highly porous material and mostly made of fiberglass, polyester felt, and cotton. The use of a breather material is dependent on the fabric-resin system and the thickness of the panel. A 2 mil (25 micron) nylon film is placed as the vacuum bag over the above. This film is placed all over the mold area and is sealed firmly using special sealant tape. The sealant seals off the vacuum bag and helps to maintain a uniform vacuum throughout the experiment. Once all of the fabrics and other relevant materials are laid over in particular sequence, the entire mold is sealed with sealant and vacuum bag. The vacuum pump is used to maintain lowest possible vacuum (in present study 0.5 torr) throughout the process. Bag leaks are the most common problems observed during the fabrication process. This may be due to damage of the nylon film before cure. Nylon film is hygroscopic and subjected to moisture changes due to changes in the moisture level in the surrounding environment. Dry and brittle film can cause cracking when it is handled too much. There is also a possibility of leaks at the nylon material and sealant interface. Once the leaks have been removed and the vacuum bag completely sealed, the vacuum pump is kep running for at least 12 hours to achieve a good vacuum in the bag. Pleating is an important step involved in the fabrication of the panel. The pleats help to avoid air pockets in the panel. The pleats go along the edges of the fabric lay up. The pleats help the mold to direct the air, if entering the mold through any of the leaks, to go through them and then subsequently through the vacuum line. The epoxy resin is mixed with hardener, and vinyl ester resin is mixed with catalyst, promoter and gel time retardant in the precalculated percentage suggested by the resin manufacturer. Before adding the resin to the mold, it has to be free of all of the air pockets that may cause voids if they enter the mold. For this purpose, the resin is mixed with the hardener in a recommended proportion and kept in a cylinder that maintains a vacuum of approximately 5 torr. This enables the suction of all the air pockets that have been trapped into the resin. Once the resin is ready, it is injected into the mold at a very slow rate. The flow of resin is controlled with the help of peristaltic pump in such a way that it is allowed to flow in the distribution medium for some distance and then the resin inlet is shut off to enable the resin to go through the thickness. This cycle is repeated until the whole panel is soaked in resin. The vacuum pump is kept running for few hours and then the mold is kept at room temperature for the next 24 hours. This is called green cure.

The correct post cure cycle has to be found for each resin to assure that the composite reaches to its optimum mechanical properties during the cure process. Figure 22 shows the curing cycle time for SC-15 resin. This cure cycle was developed with the data sheet provided by the manufacturer of the resin. The curing cycle for vinyl ester is heating at 187 ° F for 8 hours and then cooled to room temperature in the air. Figure 23 shows the overall arrangement of the fabrication process.

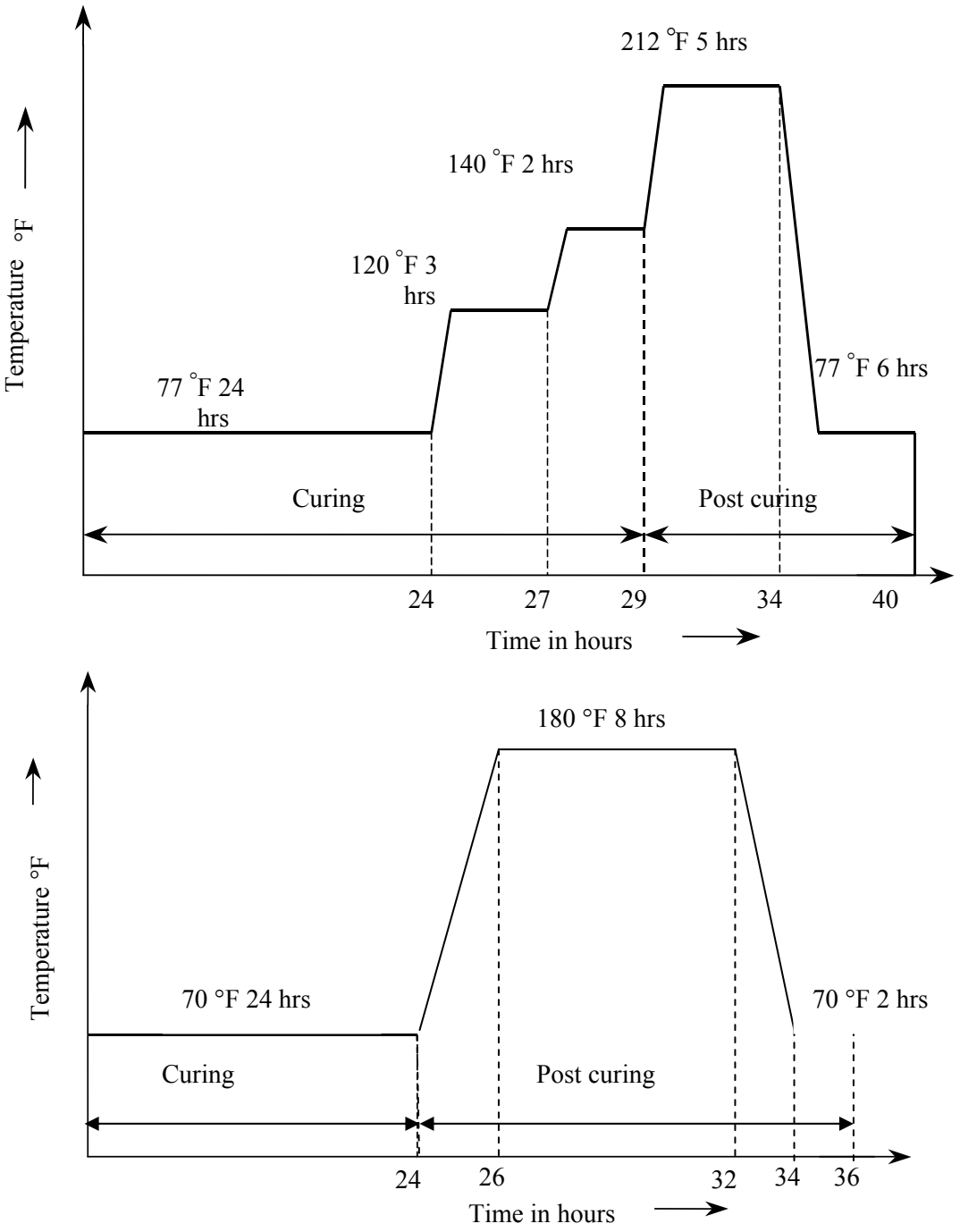

Figure 22. The Recommended Cure Cycles for SC-15 Epoxy Resin and Derakane 510 A-40 Vinyl Ester Resin

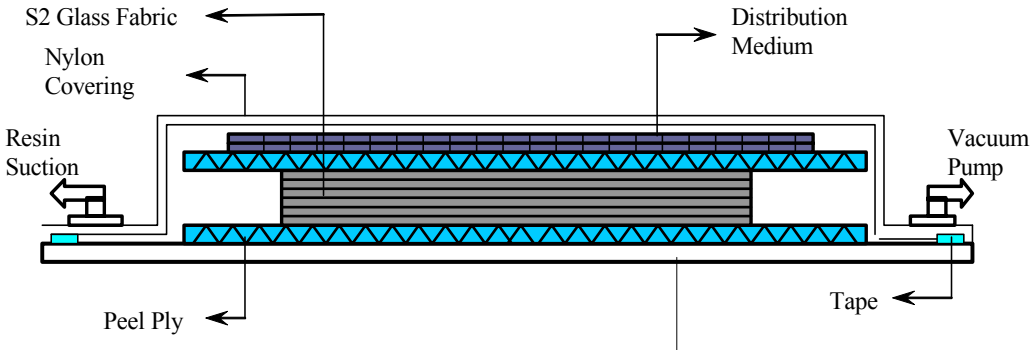

a. Side View of Panel Setup

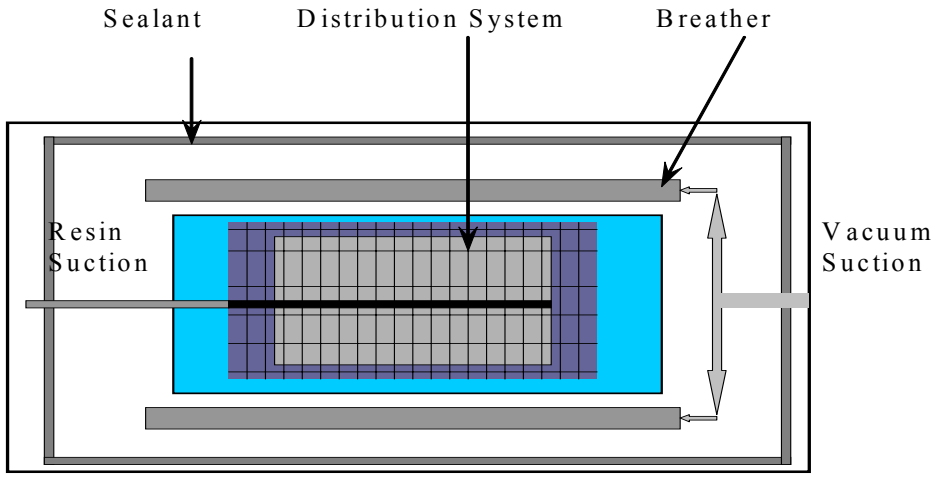

b. Top View of Panel Setup.

Figure 23. Arrangement for the Fabrication of Composite Panel

In the present fabrication, there were two set-ups used for the fabrication of the composite panels. In the first one, the main distribution channel goes on one side of the panel, and in the second set-up, the main distribution channel goes along the center of the panel. In the first set-up, the resin experiences a greater amount of resistance to flow as compared to the latter one. One of the rules of thumb is that for thick panels, the maximum distance that the resin travels should be less than 18 inches. This results in a better flow through the thickness and wets the whole of the panel before the resin reaches the gelation state. There were two approaches used in the fabrication of the panel. Both of the approaches have been shown in Figure 24 and Figure 25.

Figure 24. Approach With the Main Distributor in the Middle of the Panel

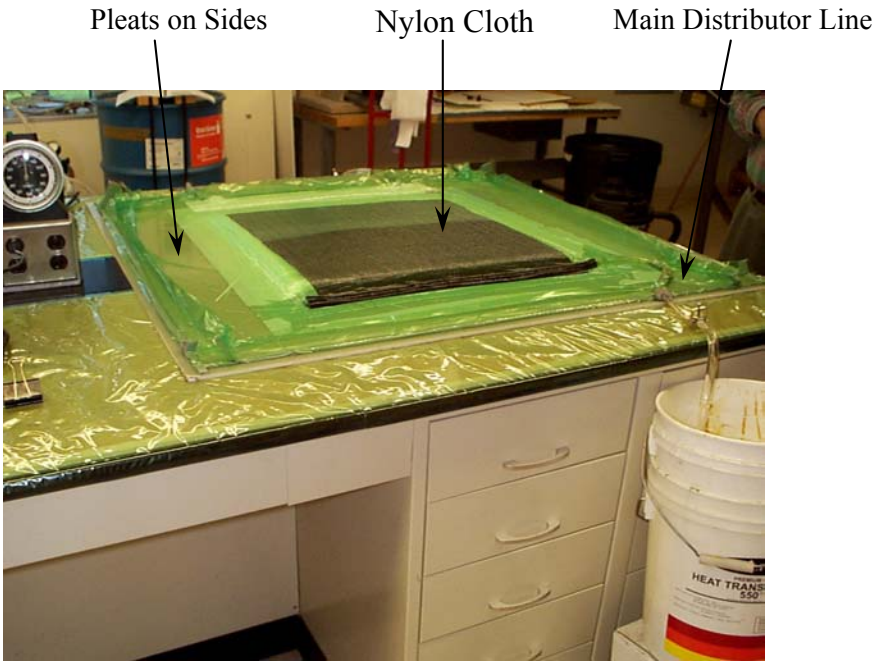

Figure 25. Approach With Distribution System in the Midsection of Panel

2.6 Impact Tests

All of the impact tests in this program will be conducted using an impact drop tower device, manufactured by DYNATUP. The low-velocity impact test facility consists of a drop tower equipped with an impactor and a variable crosshead weight arrangement, a high-speed data acquisition system, and a load transducer mounted in the impactor. The drop tower has two

different modes of testing. The first one is a gravity mode, and the second is forced velocity mode, where compressed air is used to achieve the desired velocity. In the current program, it is proposed a gravity mode be used for all low velocity impact tests. The crosshead/impactor weight will be kept constant for all tests. The low velocity impact facility is equipped with instrumentation to measure the velocity prior to impact. The high-speed data acquisition system has the capability of storing the entire impact event, and produce load-time, load-deflection, and energy-time curves.

2.6.1 Preliminary Impact Tests

The objectives of the proposed preliminary impact tests are as follows:
1. To establish the energy levels for the incipient damage threshold.
2. To establish the energy levels for the visible backface damage.

To achieve the above objectives, a series of impact tests will be performed, which are discussed in the following section.

A random drop height was selected to perform the low-velocity impact test on the woven composites. After impact, the specimens were examined for damage. The impact height was varied until the impact load-time history plots indicated no drop in impact loads due to possible impact damage in forms of delaminations. The energy level corresponding to this drop height was called the threshold energy level or lower bound. To establish the energy level for visible backface damage or the upper bound, the drop height was increased until the first visible damage was observed on the backface of the woven laminates.

Once the lower and upper bound energy levels were established, the difference between the upper and lower bound energy levels was calculated. This difference is denoted as ΔENERGY. The rest of the impact specimens will be tested at energy levels starting at approximately 20 percent of ΔENERGY, below the lower bound energy level. The energy levels were then incremented approximately 20 percent of ΔENERGY for each new specimen. This was continued until the energy level reached the upper bound.

2.6.2 Impact Test Results: Carbon/Epoxy Composites

Figure 26 shows the Load versus Impact Duration for 8-ply, 16-ply and 24-ply thick carbon/epoxy laminates. Table 9 shows that the incipient damage energy levels for 8-ply, 16-ply and 32-ply laminates are 1.52 ft-lb, 3.18 ft-lb, and 4.75 ft-lb, respectively. The upper bound energy levels were 9.48 ft-lb, 13.63 ft-lb and 47.07 ft-lb. Also, it was observed that for 8-ply laminates the maximum impact load the laminate could sustain was about 272 lbs., for 16-ply laminates about 740 lbs. and for 24-ply laminates about 1600 lbs. as shown in Table 2. It was also observed that the impact duration for thin laminates was much higher than thick laminates. The size of the specimen was 4 by 4 inches.

2.6.3 Impact Test Results: Carbon/Vinyl Ester Composites

Figure 27 shows the Load versus Impact Duration for 8-ply, 16-ply and 24-ply thick for carbon/vinyl ester laminates. Table 10 shows that the incipient damage energy levels for 8-ply, 16-ply, and 32-ply laminates are 2.588 ft-lb, 2.27 ft-lb, and 4.41 ft-lb, respectively. The upper bound energy levels were 14.726 ft-lb, 24.399 ft-lb, and 52.77 ft-lb. Also it was observed that for 8-ply laminates, the maximum impact load the laminate could sustain was about 738.40 lb, for 16-ply laminates about 1472.12 lb, and for the 24-ply laminates about 2563.21 lb, as shown in Table 3. It was also observed that the impact duration for thin laminates was much higher than thick laminates. The size of the specimen was 6 by 6 inches.

Table 9. Impact Test Data for 8-ply, 16-ply, 24-ply (Carbon/Epoxy Composites)
(Sample Size 4 by 4 Inch.)

8 Ply

Specimen No.	Drop Height, inches	Impact Velocity, ft/s	Impact Energy, ft-lb	Maximum Impact Load, lb	Impact Duration, ms
8A1	1.3	2.59	1.52	194.3	10.57
8A2	3.1	4.0	3.63	212.66	12.73
8A3	4.8	4.97	5.6	251.49	12.97
8A4	6.6	5.86	7.79	260.42	14.32
8A5(A)	8.07	6.47	9.48	273.03	15.54

16 Ply

Specimen No.	Drop Height, inches	Impact Velocity, ft/s	Impact Energy, ft-lb	Maximum Impact Load, lb	Impact Duration, ms
16A1	2.67	3.74	3.18	552.33	5.16
16A2	4.9	5.07	5.83	674.59	5.45
16A3	7.1	6.07	8.34	732.09	5.96
16A4	9.29	6.97	11.01	745.51	6.44
16A5	11.5	7.75	13.63	715.96	7.14

24 Ply

Specimen No.	Drop Height, inches	Impact Velocity, ft/s	Impact Energy, ft-lb	Maximum Impact Load, lb	Impact Duration, ms
24A1(a)	3.4	4.21	4.75	1089.24	3.8
24A2	10.75	7.51	15.09	1609.12	4.3
24A3	18.3	9.84	25.94	1559.36	5.24
24A4	26.0	11.64	36.3	1526.37	6.24
24A5	33.5	13.26	47.07	1574.94	7.38

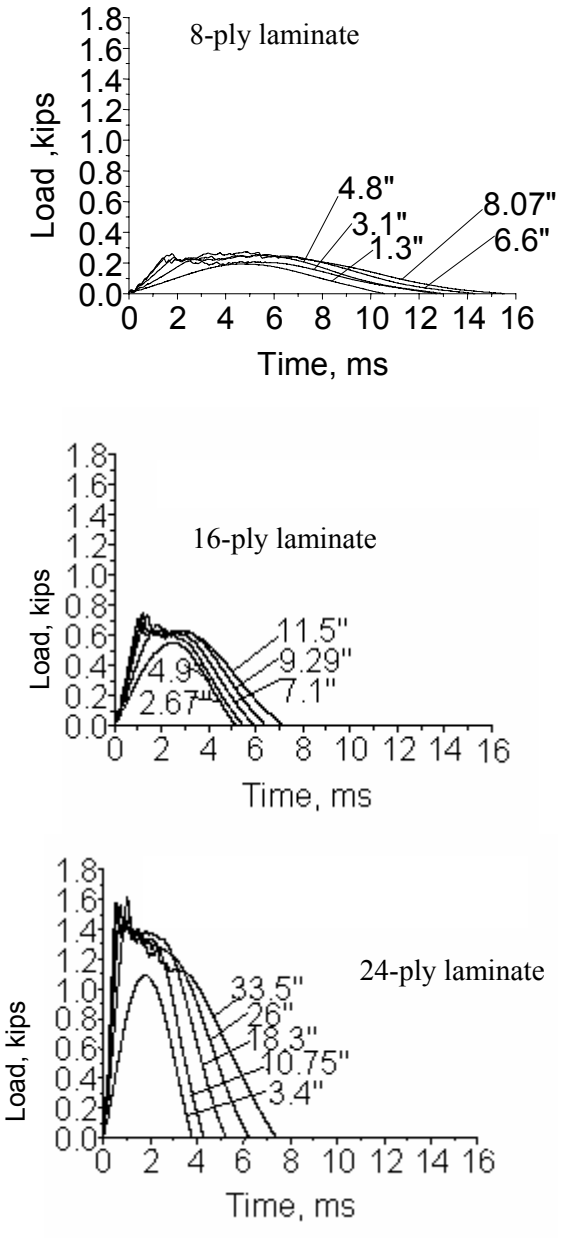

Figure 26. Impact Load Versus Time for Carbon/Epoxy Resin System
(Sample Size 4 by 4 Inch)

Table 10. Impact Test Data for 8-ply, 16-ply, 24-ply Carbon/Vinyl Ester Composites (Size of Specimen 6 inch by 6 inch)

8-ply

Specimen No.	Drop Height, inches	Impact Velocity, ft/s	Impact Energy, ft-lb	Maximum Impact Load, lb	Impact Duration, ms
8p_2in	2	3.58	2.588	297.69	9.206
8p_4in	4	4.86	4.626	473.50	12.30
8p_6in	6	5.73	6.379	567.53	13.59
8p_8in	8	6.69	8.661	684.32	15.04
8p_10in	10	7.34	10.381	701.47	15.56
8p_12in	12	8.17	12.855	703.92	15.89
8p_14in	14	8.75	14.726	738.40	16.23

16-ply

Specimen No.	Drop Height, inches	Impact Velocity, ft/s	Impact Energy, ft-lb	Maximum Impact Load, lb	Impact Duration, ms
16p_2in	2	3.415	2.27	44.43	11.76
16p_4in	4	4.645	4.14	632.5	14.26
16p_8in	8	7.977	6.47	919.48	16.035
16p_12in	12	8.013	12.41	1176.65	16.809
16p_16in	16	9.33	16.414	1325.87	17.202
16p_20in	20	10.365	20.213	1435.80	17.472
16p_24in	24	11.389	24.399	1472.12	17.69

24-ply

Specimen No.	Drop Height, inches	Impact Velocity, ft/s	Impact Energy, ft-lb	Maximum Impact Load, lb	Impact Duration, ms
24p_2in	2”	3.24	4.41	931.31	8.27
24p_6in	6”	5.58	13.04	1673.17	8.30
24p_10in	10”	7.25	22.01	2147.61	8.40
24p_14in	14”	8.58	30.83	2481.89	8.65
24p_16in	16”	9.17	35.20	2368.01	8.79
24p_18in	18”	9.7	39.45	2657.70	8.65
24p_20in	20”	10.24	43.95	2929.16	8.62
24p_22in	22”	10.78	48.69	2441.71	10.54
24p_24in	24”	11.22	52.77	2563.21	11.30

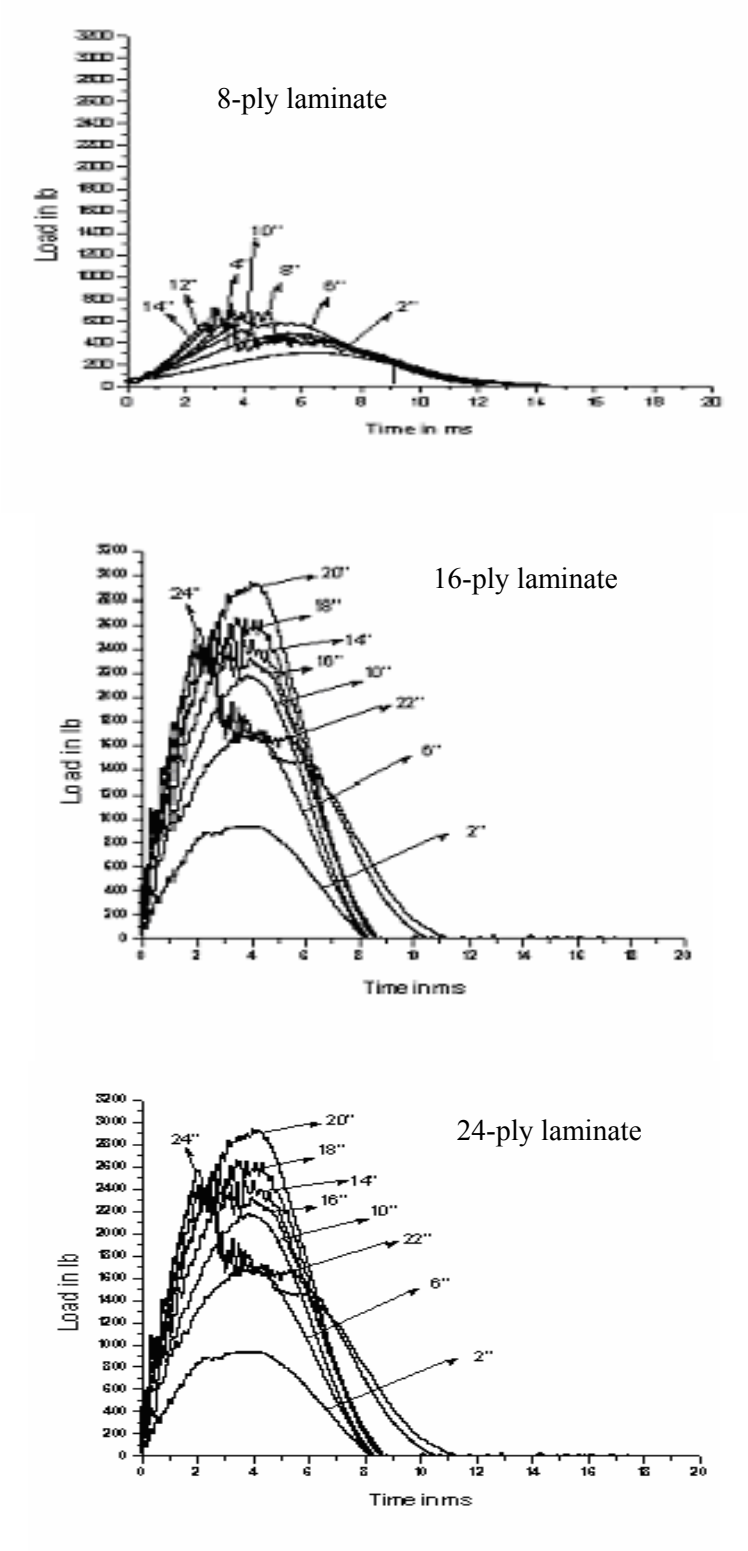

Figure 27. Impact Load Versus Time for Carbon/Vinyl Ester Resin System
(Sample Size 6 inch by 6 inch)

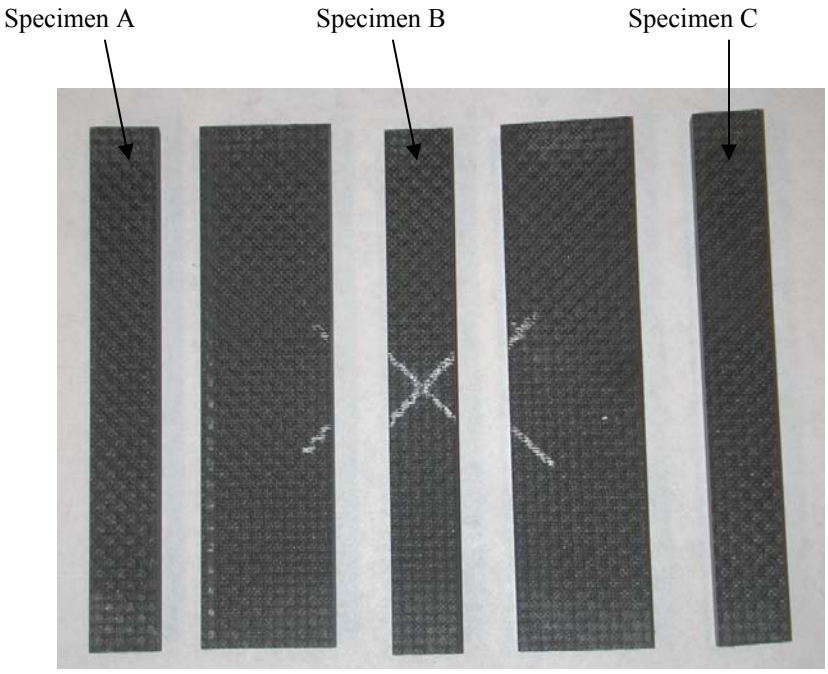

Figure 28. Impacted Sample Cut Into Compression Test Specimens

2.7 Post Impact Compression Tests (Carbon/Epoxy)

In the earlier section, the progressive damage and deformation mechanics of thin and thick woven composites subjected to low-velocity impact loading was addressed. This section presents the effect of impact damage on the stiffness of the post impacted woven laminates subjected to static compressive loading. Compressive load testing is an important tool to predict the performance of a material in actual application. It is essential to evaluate the mechanical properties of the composite before it is used in any critical application. The purpose of compressive tests is to monitor the degradation in compressive strength of the post impacted samples. This work also presents the effect of laminate thickness on the residual compressive strength.

2.7.1 Specimen Preparation

Impacted specimens are precisely cut to specific dimensions using a diamond tile saw with a diamond blade that provides a smooth cut. Rough cuts may lead to stress concentrations and in turn premature failure of specimen in the grips. Six inch by four inch impact samples are cut into five parts as shown in Figure 28. Specimens A, B, and C are 4 inches by 1 inch in size. Specimens A and C are cut at the outer edges of the impacted sample. The results from a C-scan of the impacted sample confirm that these specimens are beyond the field of impact damage. Specimen B is cut at the center of the sample where the impact occurred. The white X mark denotes the location of impact and is positioned at the center of specimen B.

2.7.2 Test Setup

Compression tests are performed using a MTS 810 Material Test System with a load frame capacity of 50 kips. A corresponding data acquisition system was manufactured by Measurements Group, Inc. and is connected to the load frame. System 5000 software also

designed by another Measurements Group; Inc. is used to design and monitor the tests. Figures 29 and 30 show the compression test set-up.

Figure 29. Load Frame for Compression Tests

Figure 30. Control Tower of Load Frame

In compression testing, it is important to avoid bending of the specimen, otherwise a wrong ultimate compressive load will be recorded. V-shaped grips, as shown in Figure 31 were used to clamp the specimens properly. The specific geometry of the grips along with the grip housing offer parallel alignment and firm gripping of the specimens. As the machine head moves to apply compressive load, the grips displace within the grip housing and thus increase the clamping force applied to the specimen. Displacement data is recorded during the movement of clamping of the specimen and movement during application of the compressive load. For this reason, strain calculations should not be based on displacement data. Figure 32 displays the lower grip housing, which has protruding rods that align with the corresponding holes in the upper grip housing. These rods assure proper alignment and hence pure axial loading.

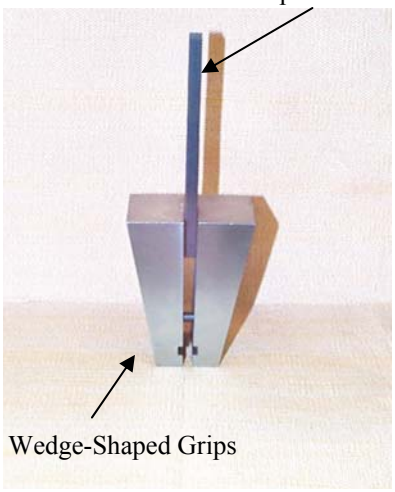

Figure 31. Compression Specimen in Grips

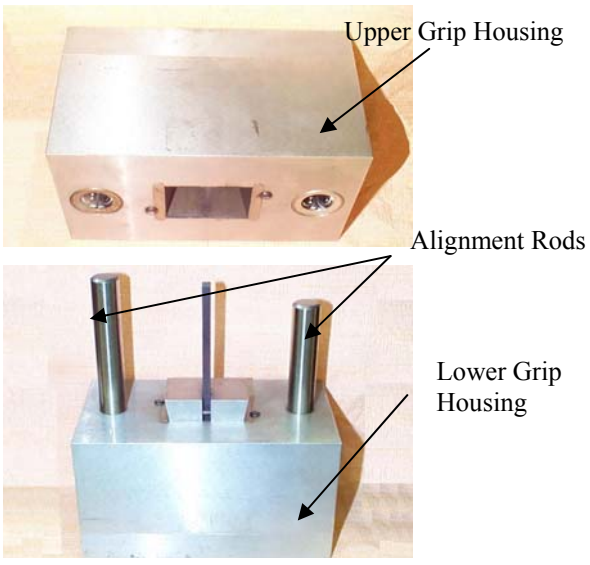

Figure 32.Compression Test Grip Housings

2.7.3 Parameters and Settings

Virgin specimen C is subjected to compression loading. The information generated from this test is implemented to establish parameters for the following compression testing of the damaged specimens of that same laminate. Compression testing is conducted on the impact-damaged specimen B from the 8-ply, 16-ply, and 24-ply composite.

2.7.4 Test Parameters

- Displacement control tests.
- Data acquisition rate: 2,000 data points/second.
- Head displacement rate: 0.02 m/min.

2.7.5 Test Procedure

The test specimen is positioned exactly vertical in the grips, thereby avoiding bending of specimen. The specimen is first clamped in the bottom grips, and then aligned with the upper grips as the lower grip housing mates with the upper grip housing. Initial clamping load is applied such that the specimen is undamaged. Excessive clamping load can damage the specimen and cause failure in the grips. Clamping load increases as lower grip displaces. Minimal preload is applied while mounting the specimen to prevent premature failure. The test is stopped when significant load drop is observed so that the specimen will not damage to the degree that failure analysis could not be predicted. The compression tests are conducted under displacement control so that the motion of the machine head can be easily controlled before additional damage occurs.

2.7.6 Compression Test Results

The maximum compressive load for each laminate is presented in Table 11 along with the corresponding drop heights. For the 8-ply laminate, the compressive load obtained was 1,836 lb. for the undamaged specimen and was decreased by 29 percent for the 1.3 inch drop height. At the final drop height of 8.07 inches, the 8-ply specimen suffered complete failure and was unable to carry any load. There is only 4.14 percent decrease in maximum compressive load between the drop heights of 7.1 inches and 9.29 inches for the 16-ply laminate. It can be concluded that at these heights, impact damage has propagated through the depth of the composite. The maximum compressive load of 6,594 lb was obtained for the 24-ply laminate when subjected to the highest drop height of 33.5 inches. Also in the 24-ply composite, a slight increase in residual compressive strength is noticed from fourth drop height of 26in to the final drop height of 33.5 inches. This behavior shows that impact damage has fully penetrated through each ply of the laminate by the fourth drop height of 26 inches and therefore the compressive response is similar to that of the specimen impacted at the next ascending drop height of 33.5 inches. In Figures 33 to 37, the behavior of each laminate in compression loading can be seen. Figure 18 demonstrates the comparison of residual compressive strength of the 8, 16, and 24-ply laminates, where the specimen with maximum impact load represents each laminate.

Table 11. Compression Tests Performance (Carbon/Epoxy Composites)

Sample	Drop Height (inches)	Max. Comp. Load (lb)	Remark
8-Ply Laminate			
8-U	N/A	1896	
8-1	1.3	1400	
8-2	3.1	984	
8-3	4.8	902	
8-4	6.6	708	
8-5	8.07	broke after impact	
16-Ply Laminate			
16-U	N/A	4643	failed in the grip
16-1	2.97	4857	
16-2	4.9	3092	
16-3	7.1	2344	
16-4	9.29	2247	
16-5	11.5	1946	
24-Ply Laminate			
24-U	N/A	6594	failed in the grip
24-1	3.4	6623	
24-2	10.75	3765	
24-3	18.3	2308	
24-4	26	2147	
24-5	33.5	2156	

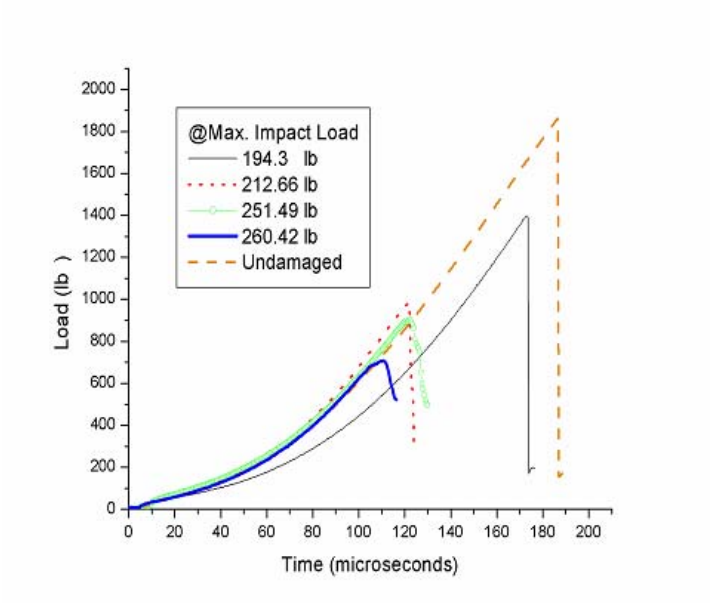

Figure 33. Compression Tests: Load Versus Time (8-ply)

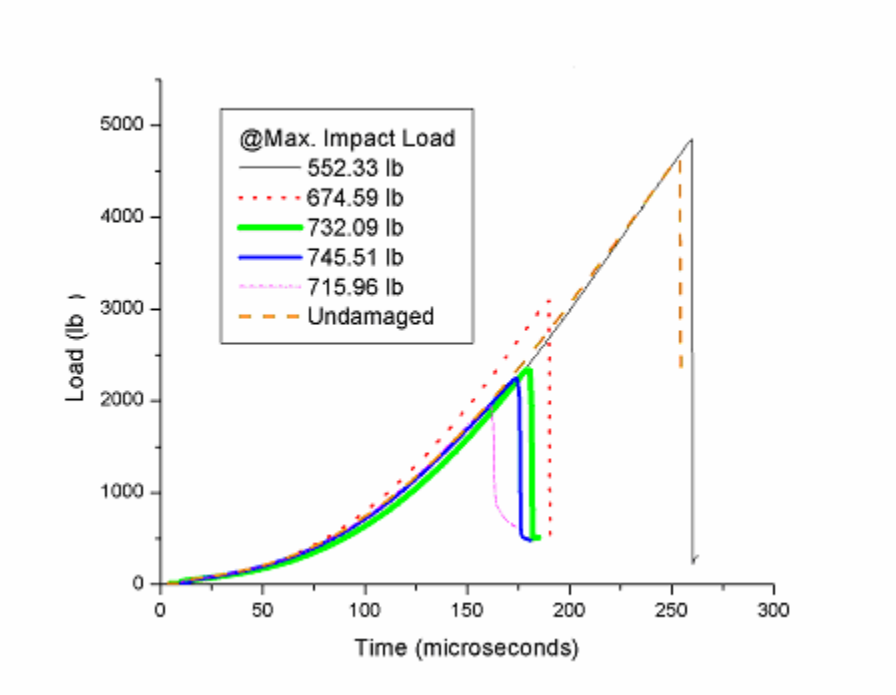

Figure 34. Compression Tests: Load Versus Time (16-ply)

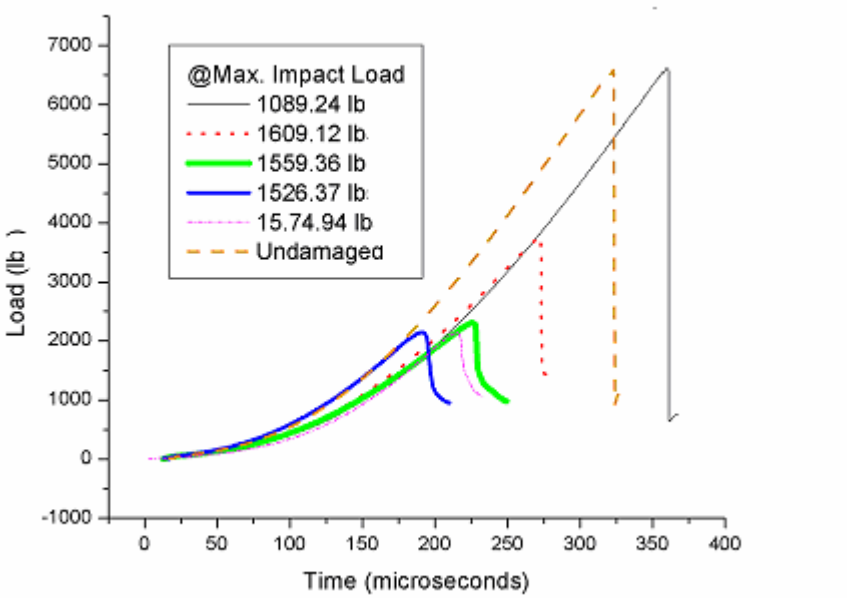

Figure 35. Compression Tests: Load Versus Time (24-ply)

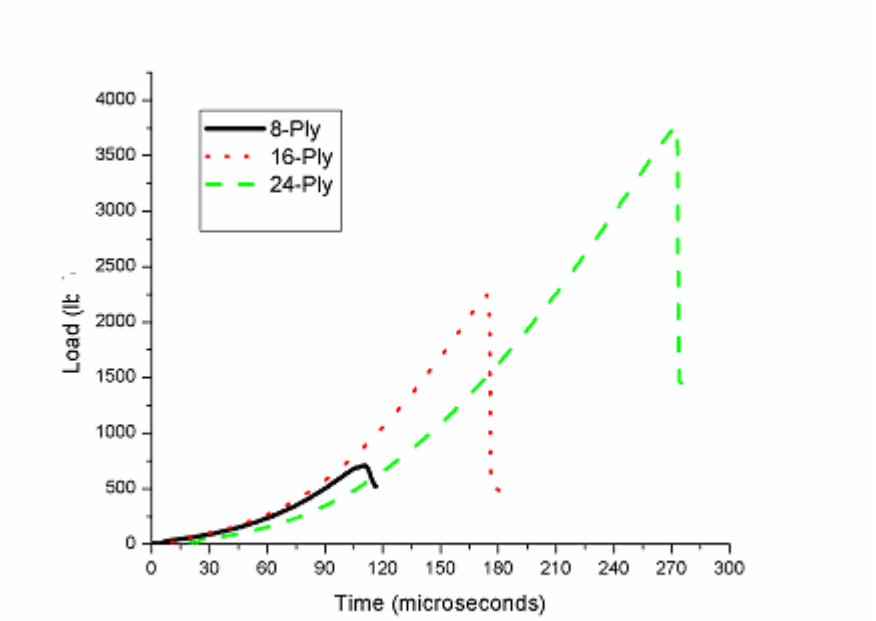

Figure 36. Compression Tests: Load Versus Time (8, 16, and 24-ply)

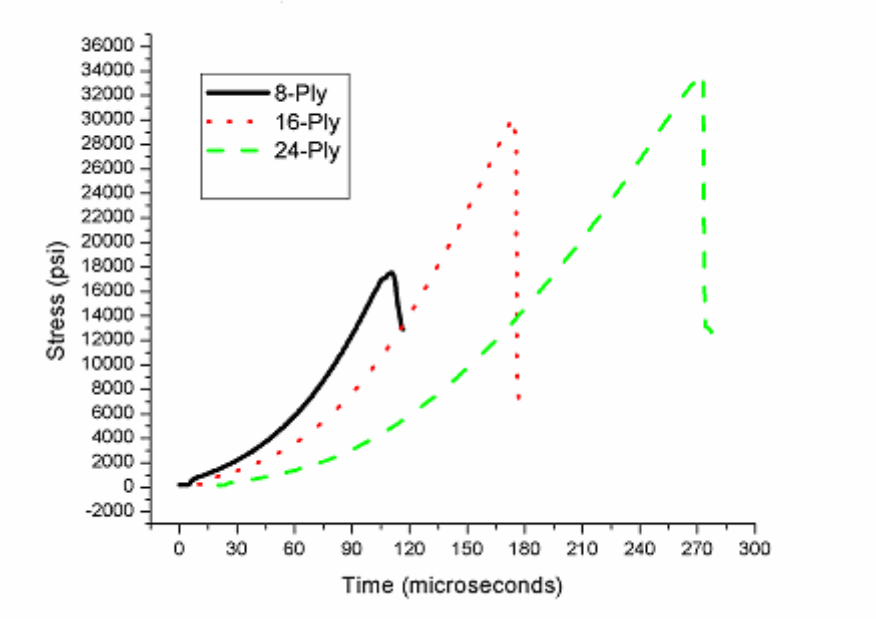

Figure 37. Compression Tests: Stress Versus. Time (8, 16, and 24-ply)

2.7.7 Failure Analysis

Beyond the effect of matrix modulus on the compressive strength of composites, the effect of fiber matrix adhesion is a factor. For polymer matrix composites, strong adhesion between fiber and matrix is important for effective load distribution. Commercially available carbon

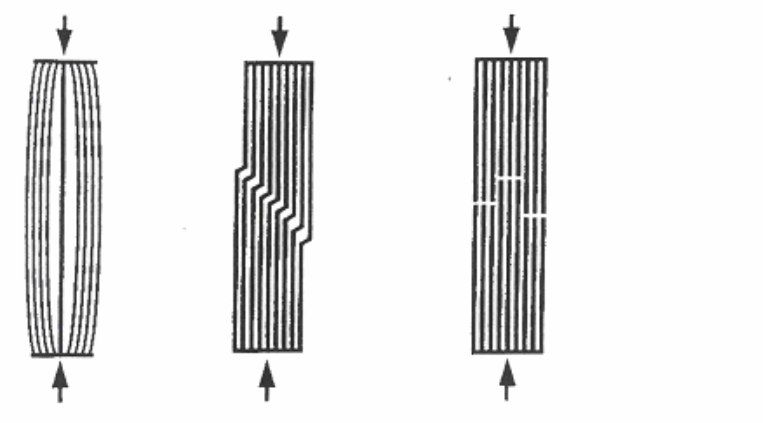

a. b. c.

Figure 38. Compressive Failure Modes of Fibers

fibers are subjected to surface treatment to ensure their compatibility with resins. Wet, dry and anionic oxidation broadly categorize the methods used to treat fibers to enhance adhesion to the matrix. Figure 38 presents the modes of compression failure of fibers in a composite. Diagram (a) represents low adhesion failure of the fibers, where the filaments delaminate from the matrix and the fibers undergo columnar buckling. Intermediate adhesion failure is displayed in diagram (b), which is representation of microbuckling along the line of maximum shear stress. In diagram (c), high adhesion failure is depicted. In this scenario, compressive failure of the fibers occurs in several planes, which results from strong lateral support to the fiber columns. It is observed that failure patterns for plain woven composites are similar to that of unidirectional composites. Figure 39 shows the means in which the composite specimens failed under compression. Photo (a) shows a failure mechanism composed of shearing and delamination. Impact damage, examined in earlier sections, is noted to propagate through the composite along the fiber direction of both 0° and 90°. The damage growth caused by this propagation influences the shear failure of the specimen. Intermediate adhesion is exhibited in photo (b), showing the occurrence of microbuckling along the line of maximum shear stress. Photo (c) represents a high adhesion condition, where failure takes place in multiple planes.

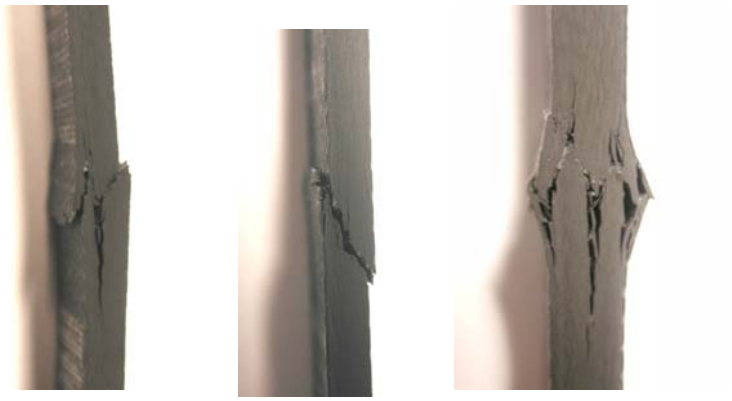

a. b. c.

Figure 39. Compressive Failure

2.8 Post Impact Fatigue Tests (Carbon/Vinyl Ester)

This section deals with the fatigue tests on 16-ply impacted specimens. The endurance limit of plain woven carbon/vinyl ester composites is about 40 percent of the ultimate tensile strength. In real life applications, the component must withstand this load even after impact loading; otherwise, the failure may be sudden and catastrophic. It is a well known fact that aircraft structures are mainly subjected to tension-tension fatigue. The maximum frequency experienced by aircraft structures is 5 Hz in adverse environmental conditions. The testing at higher frequencies can accelerate the fatigue testing and can save time. But at high frequencies, the temperature of specimen increases, which may affect the fatigue life of the specimen. Therefore, all fatigue tests on impacted specimens were performed at 40 percent of the ultimate tensile strength and are cycled for 100,000 tension-tension fatigue cycles with R ratio of 0.1 and at the frequency of 5 Hz.

2.8.1 Fatigue Tests

The stiffness degradation in fatigue-tested specimens is a function of fatigue load and the number of fatigue cycles. In this research, the fatigue load and the fatigue cycles are the same for all of the tests, which are 40 percent of the ultimate tensile strength and 100,000 fatigue cycles respectively. But these specimens are impact tested and therefore have experienced a certain amount of damage. This impact damage is going to reduce the specimen's load carrying capacity. Thus, in this study, stiffness degradation is also a function of impact drop heights. The stiffness reduces with the increase in the impact drop height. This reduction in stiffness can be an important design factor and can also be a measure of useful life prediction of the structure. With the recent advancements in NDE, it is possible to predict the stiffness of the structure and predict the useful fatigue life, which will in turn reduce the downtime and labor cost associated with it.

2.8.2 Tension Tests

The specimens are cut from the impacted samples and at the center where there is impact damage (refer to Figure 40). The size of impacted sample is 6 inches by 6 inches and the fatigue specimen is of the size 6 inches by 1 inch, which conforms to ASTM D3479 standard for tension-tension fatigue tests of polymer matrix composites. All of the specimens survived 100,000 fatigue cycles. This is positive sign that this composite can withstand the maximum impact load of 1325.87 lb (16 inch drop height) and still can survive 100,000 fatigue cycles at design stress (endurance limit).

The fatigue-tested specimens are then tested in tension at a maximum load of 3000 lb. The purpose of the tension tests is to evaluate the residual modulus of elasticity (stiffness). The axial displacements are measured with an extensometer. The results of tension tests are tabulated in the Table 12 and represented in Figure 41 in a stress-strain diagram. Figures 42 and 43 show the specimens after fatigue loading.

The modulus of elasticity reduces as the impact load increases. It is a little unusual that the nonimpacted and fatigue tested specimen 16p_f0 shows a 12.5 percent reduction in modulus.

It shows that either the endurance limit of this composite is lower than 40 percent or there is variation in fiber volume fraction from specimen to specimen. Ultimate tensile strength increases as fiber volume fraction increases. The thickness variation is unavoidable in VARTM which in turn varies with fiber volume fraction.

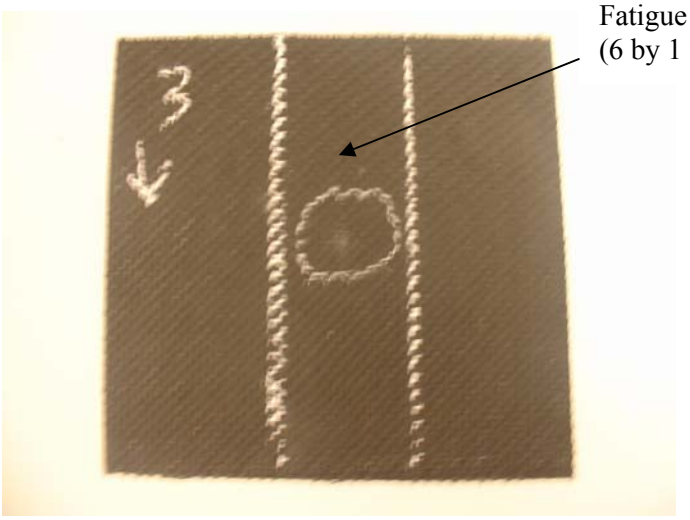

Figure 40. Impacted Sample Cut into Fatigue Specimen

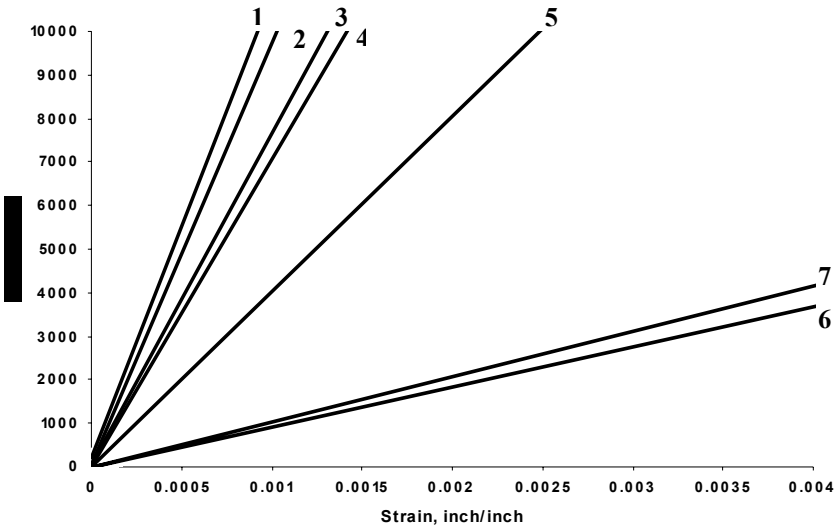

Figure 41. Stiffness Degradation of Post Impacted Specimens Tested in Tension-Tension Fatigue Loading.

Notes:

1. Virgin specimen. 2. Non impacted specimen. 3. Impacted specimen, 2 inch drop height. 4. Impacted specimen, 4 inch drop height. 5. Impacted specimen, 8 inch drop height. 6. Impacted specimen, 12 inch drop height. 7. Impacted specimen, 16 inch drop height.

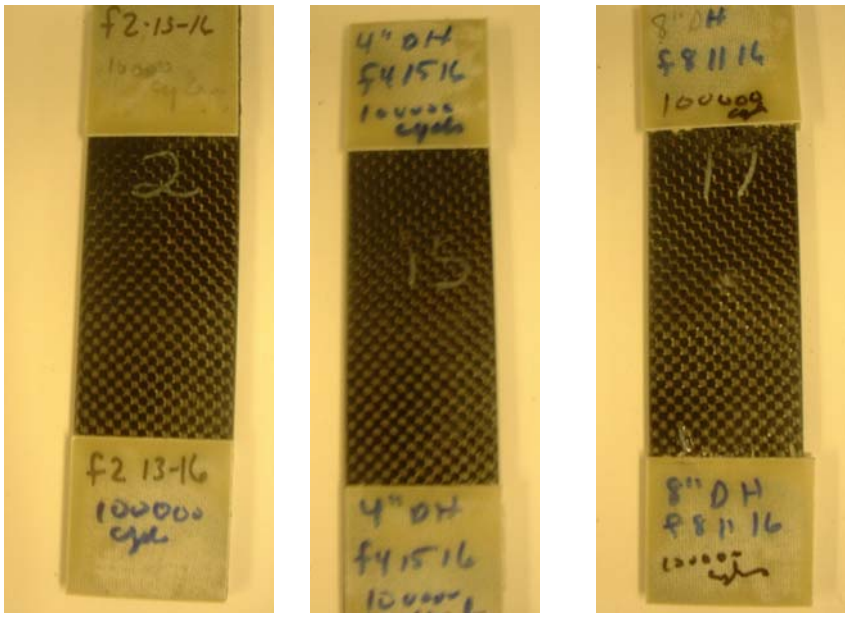

Figure 42. Fatigue-Tested Specimens Subjected to Impact Loading of 2 Inches, 4 Inches, and 8 Inches.

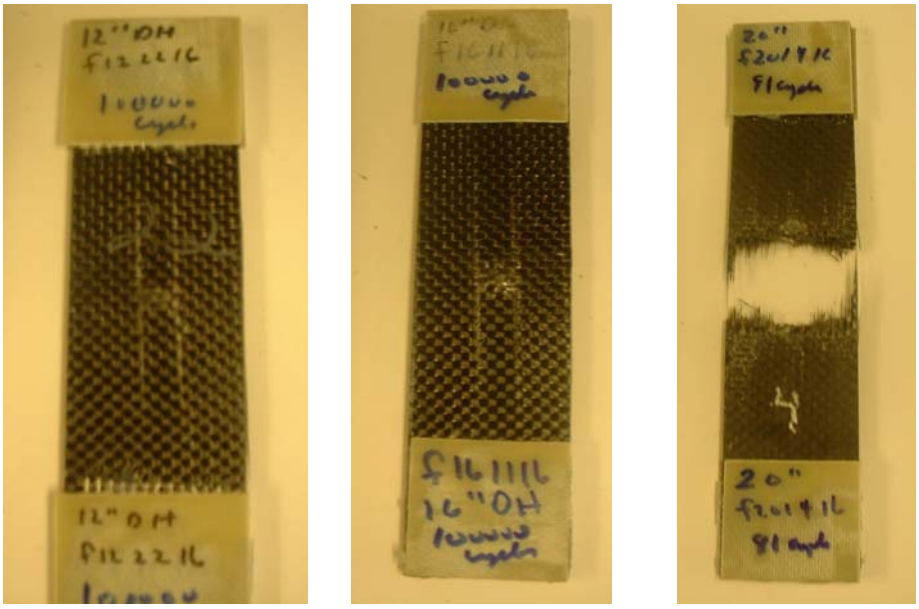

Figure 43. Fatigue Tested Specimens Subjected to Impact Loading of 12 Inches, 16 Inches, and 20 Inches.

Table 12. Stiffness Degradation of Post Impact Fatigue-Tested Specimens
(Carbon/Vinyl Ester Composites)

Specimen	Drop Height, inches	Maximum Impact Load, lb.	Number of Fatigue Cycles	Modulus of Elasticity, Msi
16p_0	0	----	0	10.69
16p_f0	0	----	100,000	9.35
16p_2in	2	44.43	100,000	7.53
16p_4in	4	632.5	100,000	6.91
16p_8in	8	919.48	100,000	3.39
16p_12in	12	1176.65	100,000	0.92
16p_16in	16	1325.87	100,000	1.00
16p_20in	20	1435.80	failed	----

2.9 Summary

In this work, low-velocity impact tests were carried out on 8-ply, 16-ply, and 24-ply carbon/epoxy and carbon/vinyl ester laminates of size 4 inches by 4 inches and 6 inches by 6 inches, respectively. The samples were subjected to impact loading using an instrumented drop-weight impact testing machine. The energy of impact was varied by varying the drop height. The impact energy for initiating damage, which is referred to as lower bound energy, and the energy level for visible back damage, which is referred to as upper bound energy level, was established. The load and energy level were functions of laminate thickness and the support dimensions. To establish the damage tolerance of woven fabric composites, post impact studies were carried out. Post impact test matrix included static compression tests and fatigue tests. Samples were subjected to static tension tests after subjecting them to fatigue cycling (100 K cycles at 40 percent of ultimate load in tension-tension mode with R= 0.1 and frequency of 5 Hz) to determine the reduction in stiffness. Though the laminates sustained the fatigue cycle, there was sharp reduction in stiffness with increasing drop height.

3. References

1. Abrate, S. "Impact on Laminated Composite Materials," *ASME Applied Mechanics Review,* Vol. 44, No. 4, pp. 155-190 (1991).
2. Cantwell, W. J. and Morton. J., "The Impact Resistance of Composite Materials - A Review," *Composites,* Vol. 22, No. 5, pp. 347-362 (1991).
3. Choi, H. Y., Wang, H. S., and Chang, F. K., "A New Approach Toward Understanding Damage Mechanisms and Mechanics of Laminated Composites Due to Low-Velocity Impact: Part I – Experiments, *Journal of Composite Materials,* Vol. 25, pp. 992-1011, (1991).
4. Greszczuk, L. B., "Damage in Composite Materials Due to Low-Velocity Impact," *Impact Dynamics,* In Zukas, Z. A. et. al. (eds.), J. Wiley, New York, pp. 55-94, (1982).
5. Elber, W., "Failure Mechanics in Low-Velocity Impacts on Thin Composite Plates," *NASA Technical Paper* 2152, (1983).
6. Wu, H. Y. and Springer, G. S., "Impact Damage of Composites," *Journal of Composite Materials,* 22, pp. 518-532, (1988).
7. Liu, S. and Chang, F. K., "Matrix Cracking Effect on Delamination Growth in Composite Laminates Induced by a Spherical Indenter," *Journal of Composite Materials,* Vol. 28, No. 10, 940-977, (1994).
8. Liu, S., "Delamination and Matrix Cracking of Cross-Ply Laminates Due to a Spherical Indenter," Composite Structures, 25, Issue 1-4, pp. 257-265, (1993).
9. Guild, F. J., Hogg, P. J., and Prichard, J. C., "A Model for the Reduction in Compressive Strength of Continuous Fibre Composites After Impact Damage," *Composites,* Vol. 24, No. 4, pp. 333-339, (1993).
10. Hull, D. and Shi, Y. B., "Damage Mechanism Characterization in Composite Damage Tolerance Investigations," *Composite Structures,* Vol. 23, No. 2, pp. 99-120, (1993).
11. Prichard, J. C., and Hogg, P. J., "The Role of Impact Damage in Post-Impact Compression Testing," *Composites,* Vol. 21, No. 6, pp. 503-511, (1990).
12. Chen, V. L., Wu, H. Y. T., and Yey, H. Y., "A Parametric Study of Residual Strength and Stiffness for Impact Damage Composites," *Composite Structures*, Vol. 25, No. 1-4, pp. 267-275, (1993).
13. Hosur, M. V., Murthy, C. R. L., and Ramamurthy. T. S., "Compression After Impact Testing of Carbon Fiber Reinforced Plastic Laminates," *Journal of Composites Technology and Research,* pp. 51-64, (1999).
14. Huang, S.L., Richey, R. J., and Deska, E.W., "Cross-Reinforcement in a GFRP Laminate," Paper presented at ASME, Winter Annual meeting, San Francisco, USA, (1978).
15. Mignery, L. A., Sun, C. T., and Tan, T. M., "The Use of Stitching to Suppress Delamination in Laminated Composites," *ASTM STP 876,* pp. 371-385, (1985).
16. Kang, T. J., and Lee. S. H., "Effect of Stitching on the Mechanical and Impact Properties of Woven Laminate Composite," *Journal of Composite Materials,* Vol. 28, No. 16, pp. 1574-1587, (1994).
17. Dransfield, K., Baillie, C., and Mai, Y. M., "Improving the Delamination Resistance of CFRP by Stitching – Review," Composites Science & Technology, Vol. 50, No. 3, pp. 305-317, (1994).
18. Mouritz, A. P., and Cox, B. N., "A Mechanistic Approach to the Properties of Stitched Laminates," *Composites Part A: Applied Science and Manufacturing,* Vol. 31, No. 1, pp. 1-27, (2000).

19. Mouritz, A. P, Leong, K. H., and Herszberg, I., Composites *Part A: Applied Science and Manufacturing,* 28, pp. No. 12, 979-991, (1997).
20. Su, K. B., "Delamination Resistance of Stitched Thermoplastic Matrix Composite Laminates," *ASTM STP 1044,* pp. 279–300, (1989).
21. Jain, L. K., and Mai, Y. W. 1995. "Determination of Mode II Delamination Toughness of Stitched Laminated Composites," Composites Science and Technology, Vol. 55, No. 3., 241-253.
22. Shu, D. W. Mai, Y. W. "Effect of Stitching on Interlaminar Delamination Extension in Composite Laminates," *Composites Science and Technology,* Vol. 49, No. 2, 165-171.
23. Farley, G. L., Smith, B. T., and Maiden, J., "Compression Response of Thick Layer Composite Laminates With Through-The-Thickness Reinforcement," *J. Reinforced Plastics and Composites* Vol. 11, pp. 787–810, (1992).
24. Liu, D. "Delamination Resistance in Stitched and Unstitched Composite Planes Subjected to Composite Loading," Journal of Reinforced Plastics and Composites, Vol. 9, No. 1, 59-69.
25. Pelstring, R. M., and Madan, R. C., Stitching to Improve Damage Tolerance of Composites. In: *Proc. 24th Int. SAMPE Symp.,* pp. 1519–1529, (8–11 May 1989).
26. Taylor, A., "RTM Material Developments for Improved Processability and Performance," *SAMPE Journal,* Vol. 36, No. 4, (July/August 2000).
27. Faiz, R., "Net RTM Preforming Process for Cost Effective Manufacturing of Military Ground Vehicle Composite Structures," *Proc. 28th Int. SAMPE Symp.,* pp. 381-292, (1996).
28. Schwartz, M. M. "Composite Materials - Processing, Fabrication and Applications," Prentice-Hall Publishers, Vol. II, (1996).
29. Wu, E. and Chang, L. C., "Loading Rate Effect on Woven Glass Laminated Plates by Penetration Force," Journal *of Composite Materials,* Vol. 32, No. 8, pp. 702-721, (1998).
30. Naik, N. K., and Chandra Sekher, Y., "Damage in Laminated Composites due to Low-Velocity Impact," *Journal of Reinforced Plastics and Composites,* Vol. 17, No. 14, 1222-1263, (1998).
31. Naik, N. K., Chandra Sekher, Y., and Meduri, S., "Polymer Matrix Woven Fabric Composites Subjected to Low-Velocity Impact" Part I – Damage Initiation Studies," *Journal of Reinforced Plastics and Composites,* Vol. 19, No. 12, 912-954, (2000).
32. Naik, N. K., Chandra Sekher, Y., and Meduri, S., "Polymer Matrix Woven Fabric Composites Subjected to Low-Velocity Impact" Part II – Effect of Plate Thickness," *Journal of Reinforced Plastics and Composites,* Vol. 19, No. 13, 1031-1054, (2000).
33. Walsh, T. F., Lee, B. L., and Song, J. W., "Penetration Failure Mechanisms of Woven Textile Composite," *Proceedings for the American Society for Composites,* Atlanta, GA, pp. 979-988, (1996).
34. Ishikawa, T., and Chou, T.W., "Stiffness and Strength Behavior of Woven Fabric Composites", *Journal of Material Science,* Vol. 17, pp 3211-3220, (1982)
35. Ishikawa, T., Chou, T.W., "Elastic Behavior of Woven Hybrid Composites", *Journal of Composite Materials,* Vol. 16, pp 2-19, (1982).
36. Naik, N. K., Ganesh, V. K., "Prediction of On-Axes Elastic Properties of Plain Weave Fabric Composites", *Composites Science and Technology,* Vol. 45, pp 135-152, (1992).
37. Whitcomb, J., "Three-Dimensional Stress Analysis of Plain Weave Composites," *Composite Materials: Fatigue and Fracture (Third Volume), ASTM STP 1110*, O'Brien, T.K. ed., pp 417-438, (1991).
38. Whitcomb, J., Srirengan, K., "Effect of Various Approximations on Predicted Progressive Failure in Plain Weave Composites," Composite Structures, *Composite Structures,* Vol. 34, Issue 1, pp. 13-20, (1995).

39. Espinosa, H. D., Lu, H. Xu., and Yueping, "Novel Technique for Penetrator Velocity Measurement and Damage Identification in Ballistic Penetration Experiments," Journal of Composite Materials, Vol. 32, No. No. 8, pp. 722-743, (1998).
40. Navarro, C., **"**Modeling of High Velocity Impact on Woven Fabrics and Composite Materials," *Metal Matrix Composites Proceedings of the 9th International Conference on Composite Materials,* ICCM/9, Madrid, Spain, Part 1 (of 6) Vol. 1, pp. 131, (1993).
41. Navarro, C., Rodriguez, J., and Cortes, R., "Analytical Modeling of Composite Panels Subjected to Impact Loading," *Journal De Physique* Proceedings of the International Conference on Mechanical and Physical Behavior of Materials under Dynamic Loading, Vol. 4, No. 8, pp. 515-520, (1994).
42. Mahfuz, H., Saha, M., Biggs, R., and Jeelani, S., "Damage Tolerance of Resin Infiltrated Composites Under Low Velocity Impact - Experimental and Numerical Studies," *Key Engineering Materials,* Vol. 141-143, No. Pt 1, pp. 209-234, (1998).

List of Acronyms

Acronym	Description
CFRP	carbon fiber-reinforced plastic
FRP	fiber-reinforced plastic
NDE	nondestructive evaluation
RH	relative humidity
RTM	resin transfer molding
SEM	scanning electron micrograph (or microscope or microscopy)
VARIM	vacuum assisted resin infusion molding
VARTM	vacuum assisted resin transfer molding